

Chapter 6

Z-Selective Ruthenium Metathesis Catalysts

The text in this chapter is reproduced in part with permission from:

Keitz, B. K.; Endo, K.; Herbert, M. B.; Grubbs, R. H. *J. Am. Chem. Soc.* **2011**, 133, 9686.

Keitz, B. K.; Endo, K.; Patel, P. R.; Herbert, M. B.; Grubbs, R. H. *J. Am. Chem. Soc.* **2012**, 134, 693.

Keitz, B. K.; Fedorov, A.; Grubbs, R. H. *J. Am. Chem. Soc.* **2012**, 134, 2040.

Copyright 2011 and 2012 American Chemical Society

Abstract

The preparation of C-H-activated ruthenium (Ru) metathesis catalysts for Z-selective olefin metathesis is described. Both the carboxylate ligand and the aryl group of the N-heterocyclic carbene (NHC) ligand have been altered and the resulting catalysts were evaluated using a range of metathesis reactions, including cross metathesis (CM) and ring-opening metathesis polymerization (ROMP). Furthermore, the effect of various ligands on catalyst stability is also discussed along with several unique decomposition structures.

Replacement of the carboxylate ligand on the C-H-activated catalyst with a nitrate group (NO_3^-) resulted in a catalyst with improved activity, selectivity, and tolerance to dioxygen (O_2). This catalyst was found to be capable of ca. 1000 turnovers (TON) with Z-selectivities above 90% in homodimerization reactions.

Introduction

As discussed in Chapter 1, olefin metathesis is a thermodynamically controlled reaction, meaning that there is an equilibrium between the starting materials and the products of a reaction.¹ Moreover, it is well established that in most cases, the *trans* or *E*-olefin is thermodynamically preferred.² Consequently, olefin metathesis gives a higher percentage of *E*-olefins compared to *cis* or *Z*-olefins (Figure 6.1). In order to overcome this limitation and prepare *Z*-olefins via metathesis, chemists have adopted two strategies. One strategy relies on the use of specially designed substrates that yield *Z*-olefins upon metathesis and deprotection.⁴ The other strategy relies on the design of catalysts that are kinetically

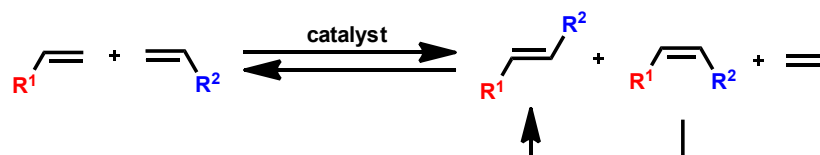


Figure 6.1. Conversion of Z- to E-olefin under thermodynamic control

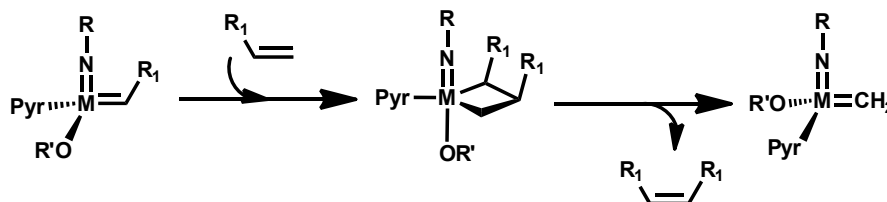


Figure 6.2. Mechanism of Z-selective olefin formation in Mo and W MAP catalysts³

selective for Z-olefins. The preparation of such a catalyst has been extremely challenging since the catalyst must not only be initially selective for Z-olefins but also must not convert Z-olefins into *E*-olefins via secondary metathesis. Recently, the Schrock and Hoveyda groups reported the first examples of Z-selective olefin metathesis using monoalkoxide pyrrolide (MAP) tungsten (W) and molybdenum (Mo) catalysts.³ These catalysts are effective because they operate through well-defined metallacycle intermediates, the geometry of which is strongly influenced by the pyrrolide and alkoxide ligands (Figure 6.2). In contrast, metathesis-relevant ruthenacycles are much less well defined and have never been characterized by x-ray crystallography.⁵ Moreover, as was shown in Chapter 5, they are also highly fluxional species, even at cryogenic temperatures. For these reasons, and because extremely large ligands shut down Ru activity, a Ru-based analog of the Z-olefin selective Mo and W catalysts has remained out of reach.

However, we recently reported on the synthesis of a C-H-activated Ru metathesis catalyst where the N-heterocyclic carbene (NHC) is chelated to the

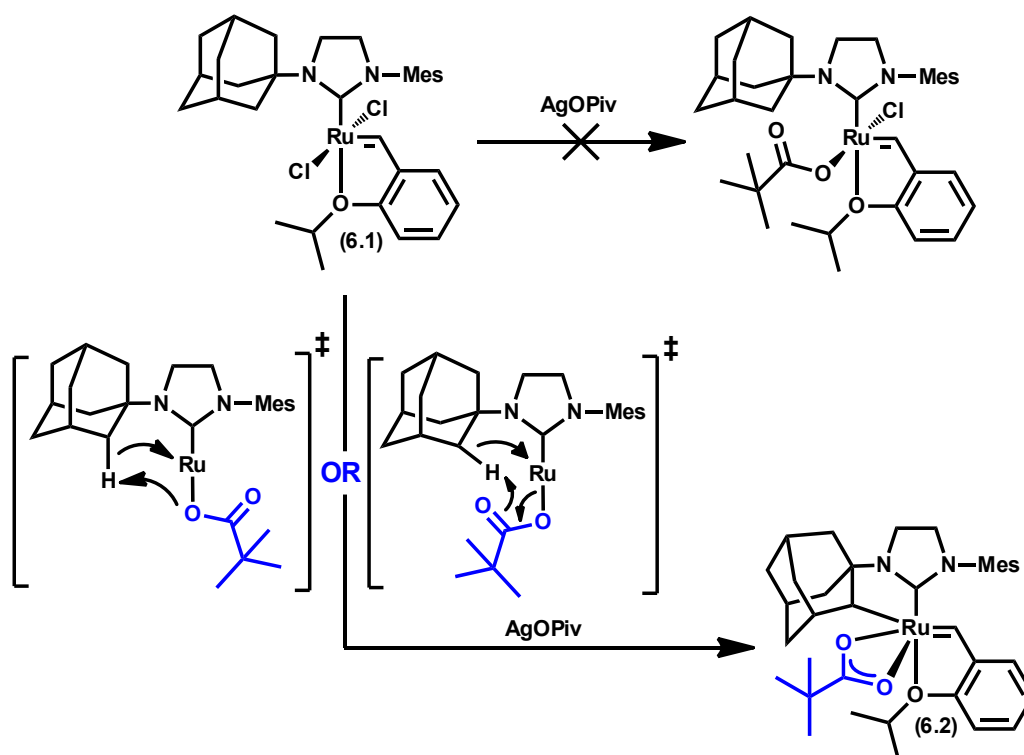


Figure 6.3. Carboxylate-induced C-H activation of **6.1** to form Z-selective catalysts **6.2**

metal center through a Ru-C bond (Figure 6.3).⁶ The unique carboxylate-induced C-H-activation reaction responsible for the generation of the Ru-C bond effectively bypasses the generation of an unstable Ru-H (hydride) species and subsequent decomposition.⁷ Structural analogs of **6.2** have been previously isolated, but were always the result of catalyst decomposition and were never metathesis active themselves. Thus, it was surprising when **6.2** was found to be active at both ring-opening metathesis polymerization (ROMP) and ring-closing metathesis (RCM). More surprising was the fact that **6.2** exhibited remarkable selectivity for Z-olefins during the cross-metathesis of allylbenzene (**6.3**) with *cis*-1,4-diacetoxy-2-butene (**6.4**).⁶

In this chapter, we describe the optimization of **6.2** for the Z-selective

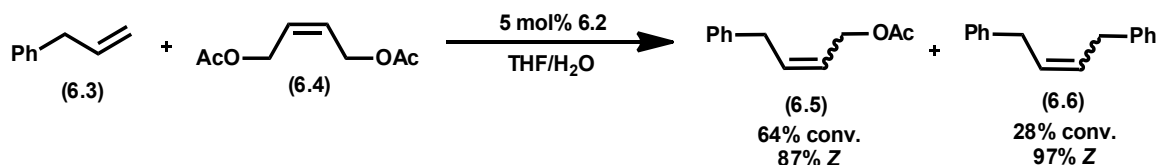


Figure 6.4. Previously reported Z-selectivity of **6.2**

homodimerization of terminal olefins and detail structural changes that have improved the activity and stability of **6.2** by ca. an order of magnitude. The generation of unique decomposition structures and their effect on Z-selectivity is also described. Finally, the application of catalysts like **6.2** towards Z-selective ROMP is discussed.

Results and Discussion

During our early attempts at the cross-metathesis of **6.3** and **6.4**, we observed a significant amount of the homodimer cross-product **6.6** (Figure 6.4). However, this product was only formed in 30% yield, which corresponded to a disappointing TON of 6. Nevertheless, we reasoned that reaction conditions could be optimized to provide good yields of **6.6** and good selectivity for the Z-isomer.

Due to the relatively large adamantyl group on **6.2** and the associative interchange initiation mechanism of complexes of this type, **6.2** required fairly high temperatures in order to initiate efficiently (ca. 70 °C).⁸ Unfortunately, cross-metathesis reactions performed at this temperature and low olefin concentration gave relatively low conversion and showed significant amounts of catalyst decomposition. We suspected that the poor performance of **6.2** under these conditions was the result of ethylene generated as a by-product of the cross-

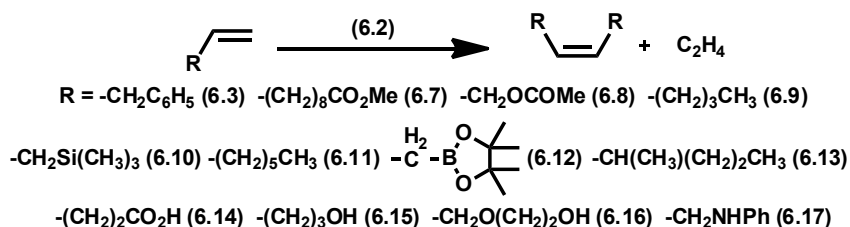


Figure 6.5. Homodimerization of terminal olefins with catalyst **6.2**

Table 6.1. Cross-metathesis of terminal olefins with **6.2** at 70 °C under static vacuum^a

substrate	Solvent	time, h	conv., ^c %	Z, ^c %
Allylbenzene (6.3)	THF	6(10)	>95 (>95)	83 (67)
Methyl undecenoate (6.7)	THF	4(6)	78 (93)	87 (85)
Allyl acetate (6.8)	THF	3(6)	53 (60)	89 (83)
1-hexene (6.9)	THF	6(7.5)	83 (87)	80 (80)
Allyl trimethylsilane (6.10)	THF	6(10)	63 (72)	>95 (>95)
1-octene (6.11)	THF	3(6)	83 (97)	80 (68)
Allyl pinacol borane (6.12)	THF	6	10	>95
3-methyl-1-hexene (6.13)	THF	12	0	0
Allyl benzene (6.6)	MeCN	2.5(21)	12 (15)	>95 (>95)
Methyl undecenoate (6.7)	MeCN	2.5(21)	7 (11)	>95 (70)

^a 2 mol% catalyst in solvent (0.6 M in substrate) at 70 °C under static vacuum. ^b 4 mol % catalyst. ^c Conversion to desired homodimer product measured by ¹H NMR spectroscopy.

metathesis reaction, and indeed, exposure of **6.2** to an atmosphere of ethylene at room temperature resulted in complete decomposition within a few minutes.

While the decomposition of **6.2** in the presence of ethylene was disappointing, it is not uncommon among metathesis catalysts and can be mitigated by the efficient removal of the gas from solution.^{8,9} Therefore, a series of cross-metathesis reactions were run under static vacuum, and under these conditions, **6.2** performed admirably (Table 6.1). For instance, **6.2** was stable in THF and MeCN as long as O₂ was rigorously excluded, and it gave high conversions and Z-selectivity for a

variety of terminal olefin substrates. Some substrates showed a slight decrease in selectivity with increasing conversion, a result which is most likely caused by decomposition products of **6.2**.¹⁰

In contrast to the Group VI metal systems, olefin migration instead of metathesis was observed in some substrates. Attempts to prevent olefin migration via the use of additives such as benzoquinone or mild acid met only with catalyst decomposition (*vide infra*).¹¹ This type of reactivity, although usually undesirable, can be valuable in certain situations.¹² Regardless, olefin migration could be eliminated via careful optimization of reaction conditions (see below). Finally, substrates with even a small amount of substitution (**6.13**) were disappointingly resistant to homodimerization, even at temperatures exceeding 100 °C.

Catalyst **6.2** is clearly functional at high temperature, the presence of deleterious side reactions encouraged us to search for conditions where **6.2** would initiate at lower temperatures. Extensive optimization revealed that **6.2** could affect the homodimerization of terminal olefins at 35 °C with high olefin concentration (ca. 3 M in substrate). This result is not surprising, considering that the initiation of **6.2** should depend on olefin concentration. Nevertheless, we did not anticipate that the activity and selectivity of **6.2** would be superior at 35 °C. Furthermore, reactions performed at lower temperature and higher concentration had the additional advantage of not requiring any special technique to remove ethylene.¹³

For most substrates, reactions with **6.2** at 35 °C showed selectivity similar to that of reactions performed at 70 °C, but improved activity (conversion, Table 6.2). Isolated yields of the homodimerization product were also good. Gratifyingly,

Table 6.2. Cross-metathesis of terminal olefins with **6.2** at 35 °C^a

substrate	time, h	conv., ^b %	Z, ^b %	yield, ^c %
Allylbenzene (6.3)	1	>95	92	81
Methyl undecenoate (6.7)	5.5	>95	73	>95
Allyl acetate (6.8)	4	>95	89	62
1-hexene (6.9) ^d	3	73	69	21
Allyl trimethylsilane (6.10)	3	>95	>95	54
1-octene (6.11)	4	>95	83	79
Allyl pinacol borane (6.12)	4	>95	>95	74
3-methyl-1-hexene (6.13)	24	0	-	-
Pentenoic acid (6.14)	24	0	-	-
4-penten-1-ol (6.15)	1	>95	72	72
2-(allyloxy)ethanol (6.16)	1	87	66	73
<i>N</i> -allylaniline (6.17)	2	70	71	67

^a 2 mol% catalyst in THF (3.33 M in substrate) at 35 °C. ^b Measured by ¹H NMR spectroscopy. ^c Isolated yield. ^d Run in sealed container.

in the case of **6.12**, no detectable amount of olefin migration was observed, and excellent Z-selectivity was maintained up to very high conversion. Emboldened by this success, we attempted to dimerize several more advanced substrates. Unfortunately, in the case of hindered or acidic substrates, no activity was observed. On the other hand, **6.2** was able to dimerize alcoholic substrates with excellent conversion and good selectivity. This latter result is particularly important since it is the first example of Z-selective cross-metathesis with alcohol substrates.

Given that **6.2** is not only stable to water and other protic media, but also shows increased activity, we deemed it appropriate to examine a wide variety of different solvents for the homodimerization of **6.3** at room temperature (RT, Table 6.3)⁶ Several polar and nonpolar solvents were tested, and the majority were conducive to the transformation. Coordinating solvents (e.g., MeCN) resulted in

Table 6.3. Solvent screen for cross-metathesis of **6.7** with **6.2** at RT^a

substrate	Solvent	time, h	conv., ^b %	Z, ^b %
Methyl undecenonate (6.7)	MeCN	3 (28)	19 (76)	94 (91)
	MeOH	3 (28)	49 (87)	88 (75)
	EtOH	3 (28)	50 (86)	89 (76)
	C ₆ H ₆	3 (21)	13 (77)	>95 (84)
	Et ₂ O	3 (7)	50 (85)	93 (73)
	DMF	3 (21)	44 (77)	92 (87)
	CH ₂ Cl ₂	3 (21)	35 (81)	93 (85)
	(CF ₃) ₂ CHOH	3 (28)	0 (0)	-
	Diglyme	3 (28)	31 (81)	95 (80)

^a 2 mol% catalyst in solvent (2.25 M in substrate) at 25 °C. ^b Measured by ¹H NMR spectroscopy.

slower reactions but were able to achieve TON roughly equivalent to those of reactions run in noncoordinating solvents. Protic solvents such as MeOH and EtOH yielded high amounts of Z-olefin product, while hexafluoroisopropanol (CF₃)₂CHOH resulted in immediate catalyst decomposition.¹⁴ The fact that high Z-selectivity is maintained in protic solvents further demonstrates the functional group compatibility of **6.2**. Nevertheless, mildly acidic substrates and solvents appear to result in catalyst decomposition.

Using **6.2**, catalyst loadings as low as 2 mol% were possible for the Z-selective homodimerization of simple terminal olefins. While these results were unprecedented for Ru-based catalysts, the observed degradation in selectivity with increasing conversion and **6.2**'s relative intolerance of dioxygen encouraged us to develop new and improved catalysts.

As previously mentioned, due to the dynamic nature of ruthenacyclobutanes,¹⁵ particularly when compared to molybdocycles and tungstacycles, the origin of the

Z-selectivity in **6.2** has remained unclear. Nonetheless, structure-function relationships derived from systematic changes of **6.2** have demonstrated that the adamantyl group in **6.2** is critical for achieving high levels of Z-selectivity.⁶ Unfortunately, our attempts to make more drastic alterations to this part of the ligand have mostly led to decomposition during the C-H activation step (*vide infra*). As a consequence of attempting to change the adamantyl group in **6.2** with little success, we turned our attention to the carboxylate ligand and to the aryl group on the NHC. Thus, exchanging the pivalate group in **6.2** for other bi- (κ^2) and monodentate (κ^1) ligands, and the mesityl for various aryl groups, has resulted in several new derivatives that yield important insight into the reactivity and selectivity of this class of catalysts. In the subsequent section, we report on the synthesis and selectivity of these new catalysts and demonstrate that several are capable of TON approaching 1000 in cross-metathesis reactions while maintaining excellent Z-selectivity.

We initiated our studies by examining a range of ligands in place of the previously reported carboxylate **6.2** (Figure 6.6). However, bulky carboxylates, such as pivalate, appear to be the only carboxylates capable of inducing the intramolecular C-H activation event necessary to form **6.2**. As such, a new synthetic route was developed in order to access analogues of **6.2** possessing different X-type ligands. We found that reacting **6.2** with NaI in THF cleanly afforded the iodo complex **6.18**, which could then be used to prepare a wide range of catalysts via transmetalation with various silver salts (Figure 6.7). Catalysts with monodentate ligands were obtained in an analogous fashion. Notably, the nitrate complex **6.24**

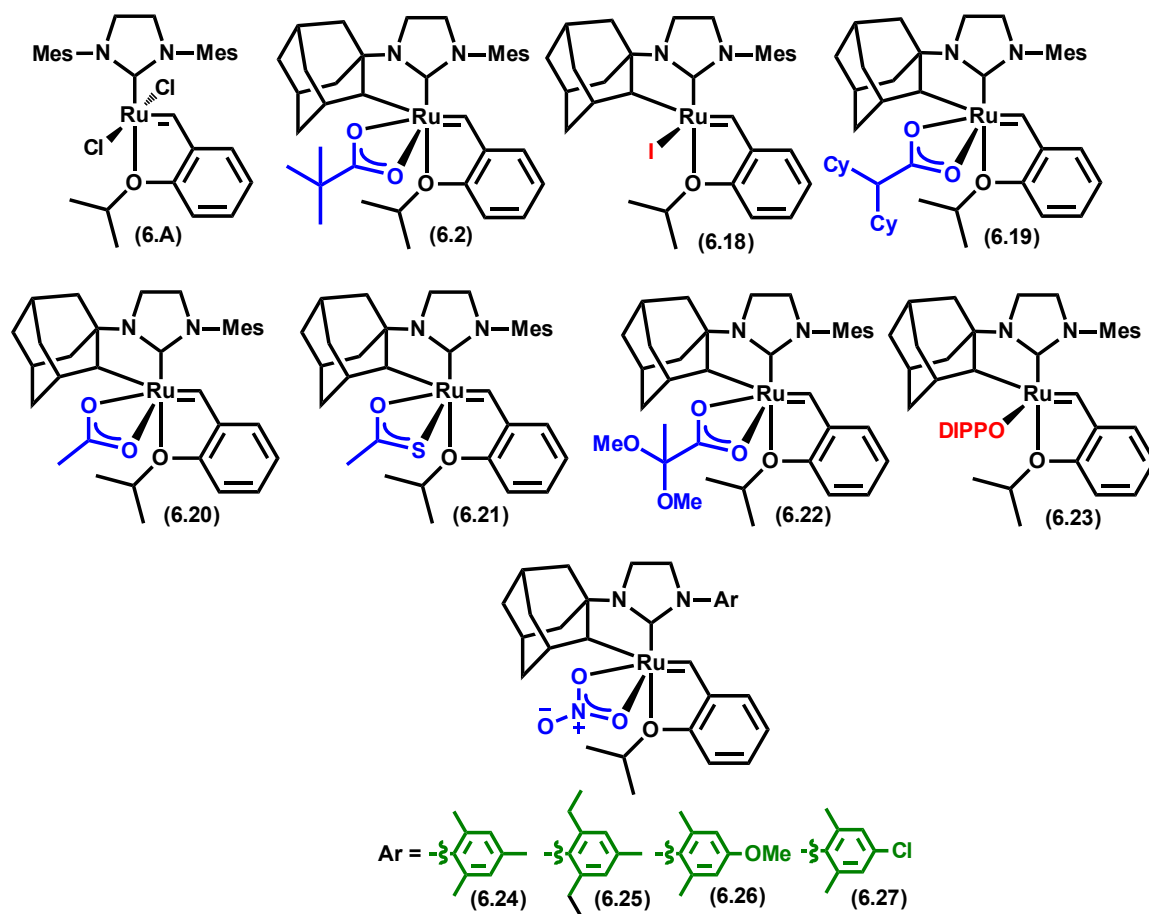


Figure 6.6. Selected variants of C-H activated catalysts. DIPP = 2,6-diisopropylphenyl

could be formed either by reaction of **6.18** with AgNO_3 or by direct reaction of **6.2** with NH_4NO_3 , with the latter route being preferred (Figure 6.8). Single-crystal x-ray diffraction revealed that the nitrate ligand in **6.24** is coordinated in a bidentate fashion analogous to **6.2** (Figure 6.9). Structural parameters, including bond lengths and angles were also consistent between **6.2** and **6.24**.

The aryl substituent on the NHC was varied through straightforward ligand synthesis, followed by metalation and C-H activation effected by silver pivalate. In all cases, the pivalate was immediately exchanged for nitrate, since the nitrate

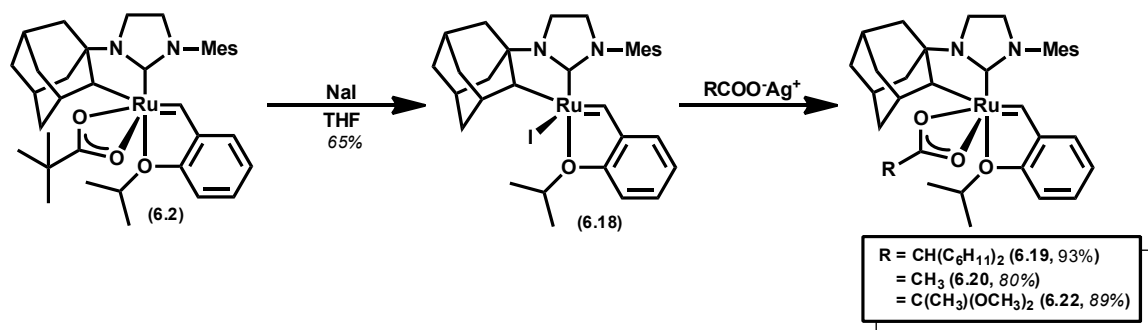


Figure 6.7. Preparation of iodo-precursor **6.18** and catalysts **6.19–6.21**

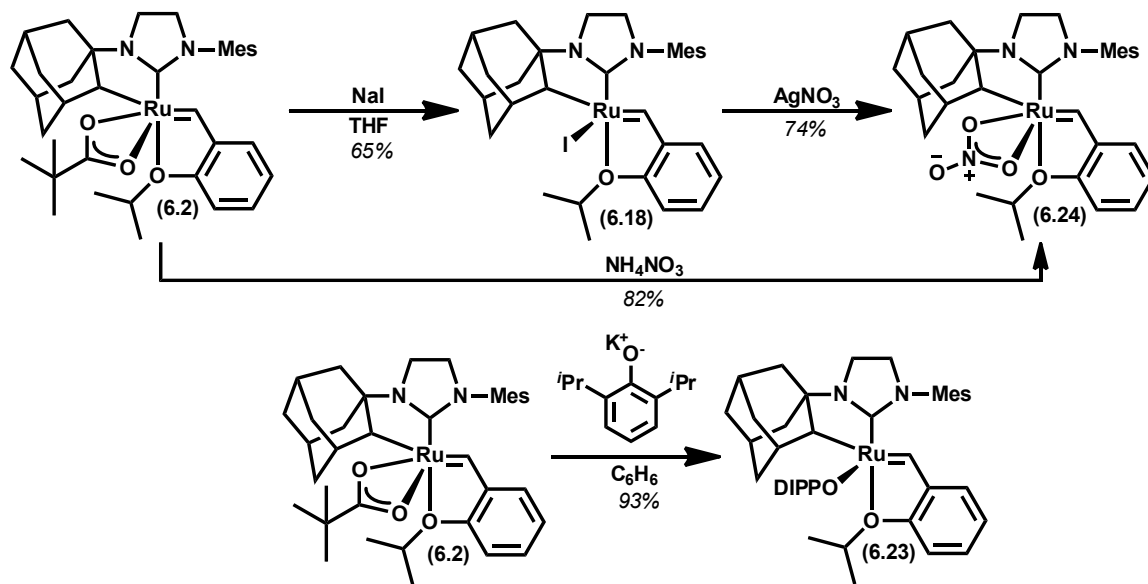


Figure 6.8. Preparation of catalysts **6.24** and **6.23**

complexes were generally more stable and easier to isolate. Only subtle steric and electronic modifications were introduced to the aryl group, as we found that the C-H activation reaction was sensitive to more drastic changes, mainly resulting in decomposition. For example, we have demonstrated that *ortho* substitution on the aryl ring appears to be necessary in order to prevent catalyst decomposition.¹⁶ Decomposition also occurred when large substituents were placed in the *meta* positions of the aryl ring (e.g., Ar = 3,5-di-*tert*-butylphenyl).¹⁷

With a relatively large library of catalysts in hand, we began examining their

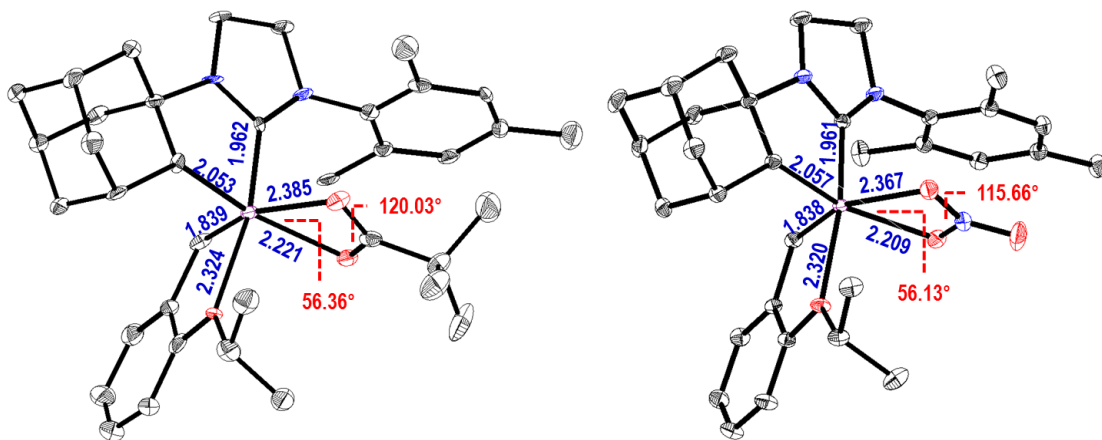


Figure 6.9. Solid state structures of **6.2** (left) and **6.24** (right) with 50% probability ellipsoids. Selected bond lengths are in Å

reactivity in a range of olefin metathesis reactions. Reaction with butyl vinyl ether (BVE) was chosen as the first probe of catalyst activity since this reaction is commonly used to measure the initiation rate of ruthenium catalysts (Figure 6.10).⁸ As shown in Table 6.4, the initiation rate constant, as measured by ¹H NMR spectroscopy, varied by 2 or more orders of magnitude for the examined catalysts! The most striking differences were observed between catalysts containing bidentate (**6.2**, **6.19–6.22**, **6.24–6.27**) and monodentate (**6.18** and **6.23**) ligands. Whereas the bidentate complexes displayed initiation rates comparable to that of **6.A**, complexes **6.2** and **6.24** initiated at significantly slower rates, even at higher temperatures. In particular, **6.23** showed almost no reactivity with BVE, even at temperatures as high as 70 °C. From these data we anticipated that the catalysts with monodentate ligands would be essentially metathesis inactive (*vide infra*).

Besides the differences between κ^1 and κ^2 ligands, several significant changes to initiation rate constant were observed between various bidentate ligands. For instance, exchanging pivalate (**6.2**) for the more inductively electron withdrawing

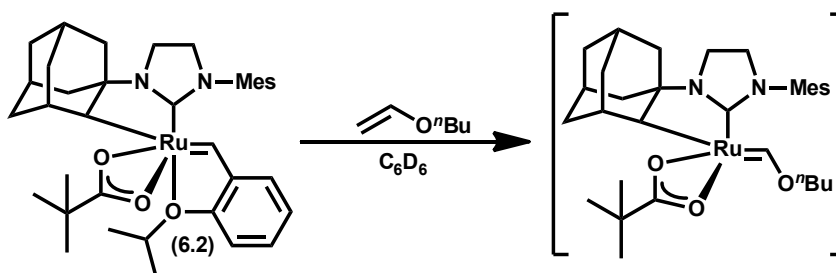


Figure 6.10. Measurement of catalyst initiation rate via reaction with BVE

Table 6.4. Initiation rate constants for C-H-activated catalysts^a

catalyst	temperature, °C	initiation rate constant, 10 ⁻³ s ⁻¹
6.A	30	7.2 ± 0.2
6.2	30	0.87 ± 0.02
6.18	50	0.17 ± 0.01
6.19	30	6.9 ± 0.3
6.20	30	0.17 ± 0.04
6.21	30	0.04 ± 0.02
6.22	30	2.5 ± 0.1
6.23	70	< 0.39 ^b
6.24	30	0.84 ± 0.03
6.25	30	0.77 ± 0.05
6.26	30	0.76 ± 0.02
6.27	30	0.24 ± 0.05

^a Initiation rate constants were determined by measuring the decrease in the benzyldiene resonance using ¹H NMR spectroscopy following addition of BVE. Conditions were catalyst (0.003 mmol) and BVE (0.09 mmol) in C₆D₆ (0.6 mL) at given temperature. ^b Value based on single half-life of **6.23**.

2,2-dimethoxypropanoate (**6.22**) led to a small increase in the rate constant. When the steric bulk of the carboxylate was increased (**6.19**) or decreased (**6.20**), initiation rate constants increased and decreased, respectively. This last result was surprising since, in general, complexes with the Hoveyda-type chelates are thought to initiate through an associative or associative interchange mechanism.⁸ Thus, increasing the steric bulk of the carboxylate should have resulted in a decrease in the initiation

rate constant due to the less favorable steric environment around the metal. The exact opposite was observed with the larger 2,2-dicyclohexylacetate (**6.19**) possessing a higher initiation rate than catalysts with smaller carboxylate ligands (**6.20**). Notably, electronic effects play an important role, as evidenced by the differences between **6.2** and **6.22**; thus, complexes of this type likely initiate through a more complicated mechanism compared to catalyst such as **6.A**. Further support for the significance of electronic effects comes from comparing **6.20** and **6.21**, which have ligands of approximately the same size, but exhibit remarkably different initiation behavior. It has been demonstrated that in some situations, thiocarboxylates tend to behave more like monodentate ligands.¹⁸ Such a result would be consistent with our observation that catalysts with monodentate ligands tend to initiate at slower rates. Finally, the nitrate complexes **6.24–6.26** had ca. the same initiation rate as **6.2**, while that of **6.27** was slightly smaller. These latter results demonstrate that minor changes to the aryl group do not have a substantial effect on initiation rate and that **6.24** and **6.2** behave almost identically in this assay.

In order to gain a better understanding of the initiation behavior of the above catalysts and to explain some of our unusual observations, we turned to more detailed kinetic studies. We first focused on steric differences, for example, between **6.20** and **6.2**. Initiation rate constants were measured at several different concentrations of BVE and the expected linear dependence was uncovered. With this same data, a double reciprocal plot was created (Figure 6.11). Assuming a dissociative mechanism (Figure 6.12), the slope and intercept of the linear fits in Figure 6.11 correspond to $k_{-1}/(k_1k_2)$ and $1/k_1$, respectively, (Eqs. 6.1 and 6.2). From

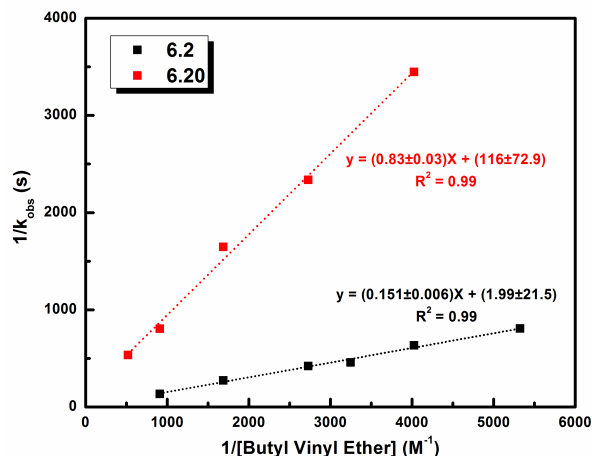


Figure 6.11. Plot of $1/k_{\text{obs}}$ versus $1/[\text{BVE}]$ for reaction of **6.2** and **6.20** with BVE

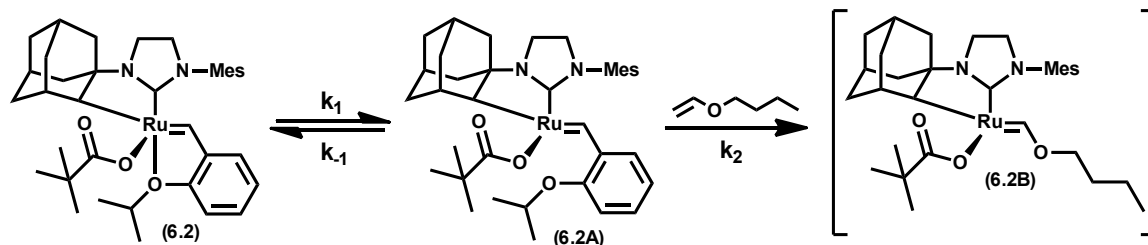


Figure 6.12. Assumed dissociation mechanism for initiation of **6.2**

$$-\frac{d[\mathbf{6.2}]}{dt} = k_2[\mathbf{6.2A}][\text{BVE}] = \frac{k_2 k_1 [\mathbf{6.2}][\text{BVE}]}{k_2 [\text{BVE}] + k_{-1}} \quad (6.1)$$

$$\frac{1}{k_{\text{obs}}} = \frac{k_2 [\text{BVE}]}{k_1 k_2 [\text{BVE}]} + \frac{k_{-1}}{k_1 k_2 [\text{BVE}]} \quad (6.2)$$

these data, k_1 and k_{-1}/k_2 were calculated (Table 6.5) and these values provide some insight into factors governing initiation. For example, k_1 , which corresponds to the dissociation of the chelated oxygen, is much larger for **6.2** than for **6.20**. This suggests that larger carboxylates (e.g., pivalate) facilitate dissociation of the chelated oxygen, which results in faster initiation rates. The values of k_{-1}/k_2 also explain the observed linear dependence on BVE concentration since the value of k_{-1} is larger or at least the same order of magnitude as $k_2[\text{BVE}]$ in the denominator of eq. 6.1, hence the linear dependence on $[\text{BVE}]$. As a disclaimer to the above

Table 6.5. Kinetic parameters for initiation of **6.2** and **6.20** with BVE^a

catalyst	k_1 , s ⁻¹	k_{-1}/k_2 , M
6.2	0.5	0.076
6.20	0.0086	0.0071

^a Derived from linear fits in Figure 6.11.

analysis, we note that we assumed a purely dissociative mechanism. This may or may not be the case depending on the reaction conditions.⁸ Nevertheless, we were able to explain some of the anomalous results from our initiation studies on catalysts with different-sized carboxylate ligands.

Having briefly examined the role of sterics in the initiation of our C-H-activated catalysts, we turned to exploring electronic effects. Several catalysts with substituted benzoate ligands were prepared and their initiation rates were measured. The resulting data was plotted as a function of an induction-based Hammett σ parameter and a positive linear response was obtained (Figure 6.13). This result indicates that inductively electron withdrawing groups (e.g., F, OH) accelerate initiation. Moreover, it also explains the larger initiation rate constant of **6.22** compared to **6.2**. At this time, it is unclear why electron withdrawing groups increase initiation rates, but the explanation may involve the ability of the bidentate ligand to switch between κ^2 and κ^1 coordination modes. Such a process has been theoretically shown to be instrumental in catalytic activity for the C-H-activated catalysts and it would not be surprising if it was affected by the electronics of the bidentate ligand.¹⁹ Unfortunately, our attempts to prepare catalysts with stronger electron withdrawing groups in order to further probe various electronic effects

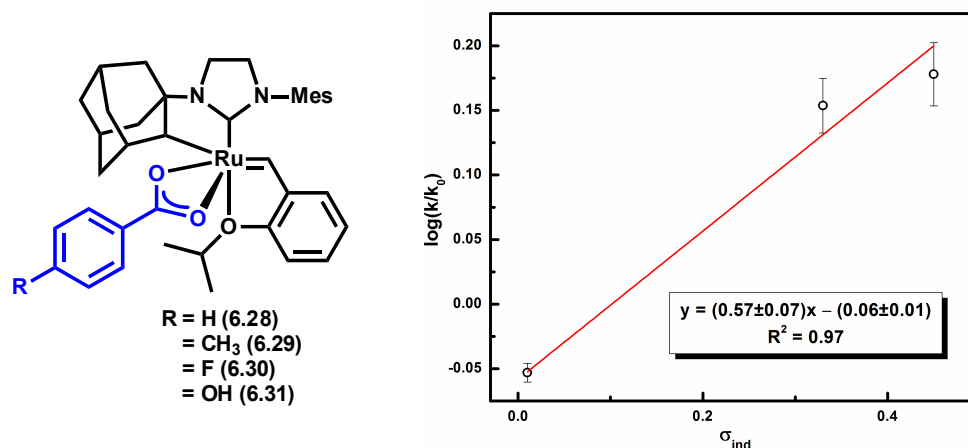


Figure 6.13. Benzoate catalysts and Hammett plot using σ induction values. Conditions were catalyst (0.003 mmol), BVE (0.09 mmol), at 50 °C^{17b}

have met only with decomposition. For example, exposure of **6.18** to AgOOCCH_3 resulted in immediate alkylidene insertion and subsequent decomposition to the Ru-olefin complex **6.32** (Figure 6.14). The identification of complex **6.32** suggests that the electronics of the X-type ligand also effect catalyst stability and not just initiation.

Our initiation studies provided insight into some subtle ligand effects, but were unable to capture the overall activity and more importantly Z-selectivity of our catalyst family. Therefore, we turned to evaluating our complexes in the cross-metathesis homocoupling of allyl benzene (**6.3**). While this reaction is relatively facile for most metathesis catalysts, it provided a useful benchmark to assess the performance of our catalyst library. Reactions were run in THF at 35 °C with a relatively high substrate concentration (ca. 3 M in **6.3**) and 0.1 mol% catalyst loading for a set amount of time, at which point the conversion and percentage of Z-olefin were measured by ¹H NMR spectroscopy (Table 6.6). Low catalyst loadings

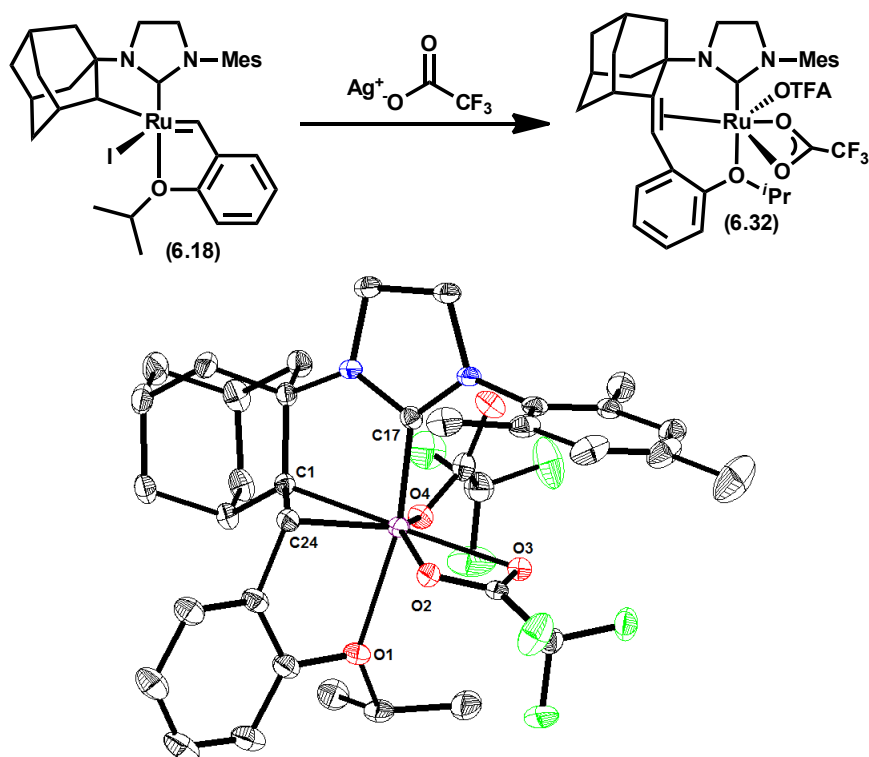


Figure 6.14. Decomposition following transmetalation with silver trifluoroacetate (AgTFA). Solid-state structure of **6.32** drawn with 50% probability ellipsoids. Selected bond lengths (Å): Ru – C1: 2.141, Ru – C17: 1.959, Ru – C24: 2.061, Ru – O1: 2.304, Ru – O2: 2.144, Ru – O3: 2.213, Ru – O4: 2.079

were used to emphasize the differences between catalysts. In most cases, a detectable amount of olefin isomerization product **6.33** was observed, but the amount of this undesired product and the total conversion of **6.3** varied significantly between catalysts. Catalysts **6.18** and **6.23** (both with monodentate ligands) yielded the largest amount of **6.33**; moreover, this was the only detectable product for these catalysts. Among the carboxylate-based catalysts, **6.19** was the least active, giving low conversion of **6.3** and poor selectivity for the desired product **6.6**. Furthermore, no notable improvement was observed with complexes **6.20** and **6.22**.²⁰ Both **6.2** and **6.24–6.27** showed excellent conversion of **6.3** and good

Table 6.6. Homodimerization of allyl benzene (**6.3**)^a

C=CCc1ccccc1 (**6.3**) $\xrightarrow[\text{THF (3 M), 35 }^{\circ}\text{C}]{\text{0.1 mol\% catalyst}}$ C=CC=Cc1ccccc1 (**6.6**) + C=CC=Cc1ccccc1 (**6.33**)

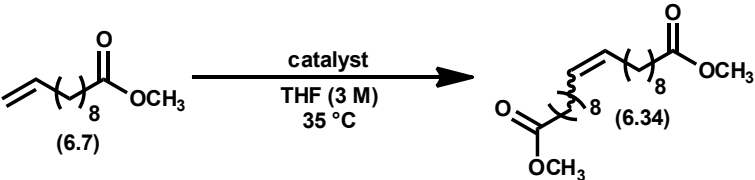
catalyst	time, h	conv., ^b %	Z- 6.6 , ^b %	13/14 ^b
6.2	3	79	> 95	42
6.18	12	59	-	0 ^c
6.19	12	7	> 95	0.5
6.20	12	65	92	1.4
6.22	12	26	> 95	3.8
6.23	12	> 95	-	0 ^c
6.24	3	90	91	18.4
6.25	3	90	93	18.1
6.26	3	91	93	16.9
6.27	3	90	94	33.6

^a Conditions were catalyst (1 μ mol) and **6.3** (1 mmol) in THF (0.2 mL) at 35 $^{\circ}$ C. ^b Measured by ^1H NMR spectroscopy. ^c No detectable amount of **6.6**

selectivity for **6.6**, with catalysts **6.24–6.27** taking only ca. 3 h to reach ~ 90% conversion. Based on the above results, the nitrate catalysts **6.24–6.27** were clearly the most efficient catalysts examined.

In order to further differentiate the performance of the catalysts, a more challenging homodimerization reaction was chosen, specifically the homodimerization of methyl 10-undecenoate (**6.7**) (Table 6.7). For this reaction, only the catalysts that performed well in the reaction with **6.3** were examined, namely the carboxylate and nitrate catalysts. We were pleased to discover that even at 0.1 mol% loading, most of the catalysts were able to achieve an appreciable degree of conversion. Similar to the reaction with **6.3**, catalysts **6.19**, **6.20**, and **6.22** performed relatively poorly while **6.2** and **6.24–6.27** furnished the best results.

Table 6.7. Homodimerization of methyl 10-undecenoate (**6.7**)^a



catalyst	loading, mol %	time, h	conv., ^b %	Z, ^b %
6.2	0.1	12	16	90
6.19	2	6	67	81
6.20	0.1	12	3	>95
6.22	0.1	12	8.4	>95

^a Conditions were catalyst (0.1–2 mol%) in THF (3 M in **6.7**) at 35 °C. ^b Determined by ¹H NMR spectroscopy

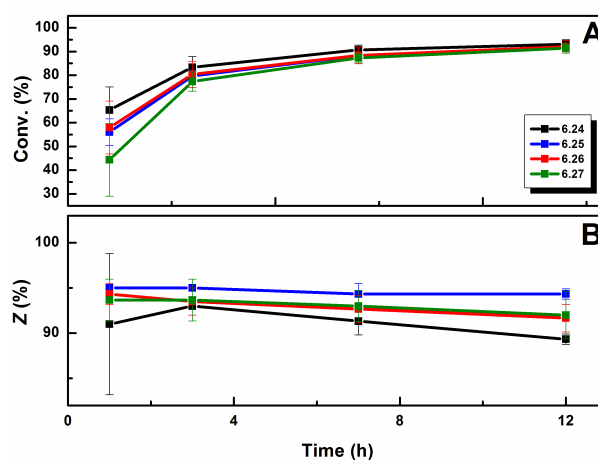


Figure 6.15. Time-course plot for the (A) conversion and (B) selectivity of the homodimerization of **6.7** to **6.34** using catalysts **6.24**–**6.27**. Conditions were **6.7** (1 mmol) and catalyst (1 μmol) in THF (0.1 mL) at 35 °C. Data points and error bars were calculated from the average and standard deviation of three separate runs

In fact, catalysts **6.24**–**6.27** showed excellent conversion (> 90%) at short reaction times with good selectivity for the Z-olefin (90–95%,). This is a clear demonstration of their superior activity and selectivity. A time-course monitoring of the reaction of **6.7** with catalysts **6.24**–**6.27** revealed some subtle differences between the nitrato catalysts (Figure 6.15). Specifically, there were only very slight differences in both

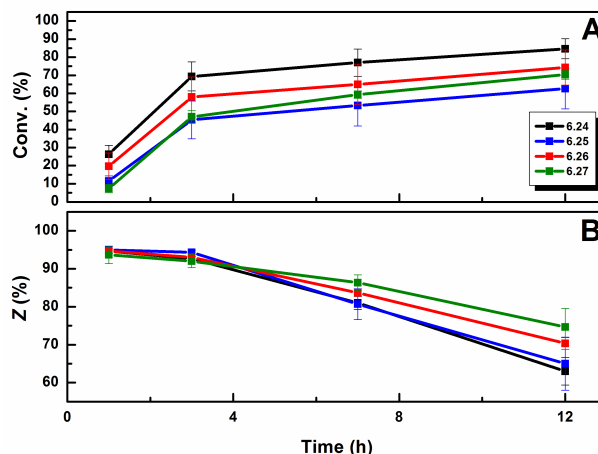


Figure 6.16. Time-course plot for the (A) conversion and (B) selectivity of the homodimerization of **6.15** to **6.34** using catalysts **6.24–6.27**. Conditions were **6.15** (1 mmol) and catalyst (1 μ mol) in THF (0.1 mL) at 35 °C. Data points and error bars were calculated from the average and standard deviation of three separate runs

conv. and Z-selectivity for catalysts **6.24–6.27** which is consistent with the initiation rate constants measured for these catalysts and their reactivity with **6.3**. At shorter reaction times, **6.27** showed slightly reduced reaction conversion compared to its analogues, which is likely a consequence of its slower initiation rate. Nonetheless, given enough time, **6.27** was able to reach similar levels of conversion as **6.24–6.26**. Similar results were achieved for the alcohol substrate **6.15** (Figure 6.16). The time-course study for **6.7** demonstrates that secondary metathesis events are relatively slow for this substrate, as Z-selectivity remains high even after extended periods of time at > 90% conversion. In contrast, secondary metathesis isomerization from Z to E-olefin appears to be faster with substrate **6.15** as evidenced by the relatively fast decrease in the Z-selectivity of the desired product.

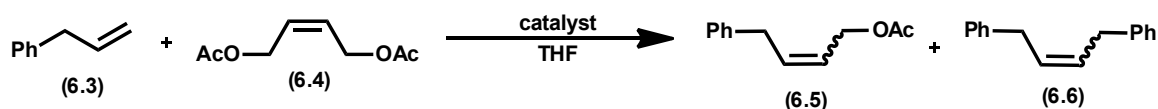
The aforementioned metathesis assays clearly demonstrated the superior

Table 6.8. Homodimerization of terminal olefin substrates^a

substrate	catalyst	time, h	Z, ^b %	yield, ^c %
6.3	6.2	3	86	73
	6.24	3	92	91
	6.25	3	94	91
	6.26	3	95	83
	6.27	3	95	89
6.7	6.2	12	90	13
	6.24	12	91	85
	6.25	12	92	94
	6.26	12	92	92
	6.27	12	94	75
6.11 1-octene	6.2	12	94	30
	6.24	12	92	83
6.15 4-penten-1-ol	6.2	12	43	81
	6.24	12	81	67
	6.25	8	73	78
	6.26	8	78	76
	6.27	8	85	75
6.8 allyl acetate	6.24	12	>95	8 ^d
6.10 allyl TMS	6.24	9	>95	14
6.12 allyl pinacol borane	6.24	3	>95	36
6.16 2-(allyloxy)ethanol	6.24	12	67	30
6.17 <i>N</i> -allylaniline	6.24	12	90	12

^a Conditions were catalyst (5 mmol) and substrate (5 mmol) in THF (ca. 1.7 mL) at 35 °C. ^b Determined by ¹H NMR spectroscopy. ^c Isolated yield after chromatography. ^d Conversion, yield not determined

properties of nitrato catalysts **6.24–6.27** over the carboxylate analogues. However, it was still unclear if this effect was specific to the chosen substrates. To fully evaluate the effectiveness of **6.24–6.27**, several more substrates, including alcohols, were examined (Table 6.8). For the majority of these reactions, catalysts **6.24–6.27** were easily capable of reaching TON greater than 500 and, in some cases, coming close to 1000. Notably, the yields presented in Table 6.8 are

Table 6.9. Cross-metathesis of **6.3** and **6.4**^a

catalyst	loading, mol%	time, h	temp, °C	conv. to 6.5 , ^b %	Z- 25 , ^b %	conv. to 6.6 , ^b %	Z- 6.6 , ^b %
6.2	5	9	70	37	89	26	>95
		6	35	50	86	19	>95
6.19	5	6	70	48	82	33	91
		9	35	45	87	23	>95
6.22	5	3	70	57	75	42	94
		6	35	64	79	22	>95
6.20	5	7	35	54	83	17	>95
6.24	1	9	35	58	91	28	>95

^a Conditions were catalyst, **6.3** (1 equiv) and **6.4** (2 equiv) in THF (0.5 M in **6.3**). ^b Determined by gas chromatography with tridecane as internal standard

calculated based on *isolated yield*, meaning that the actual TON are likely to be higher. Certain substrates, such as **6.8** and **6.17** were problematic and resulted in reduced yields (TON). At this time, we believe this attenuation is not a result of the functional group itself, but of its proximity to the reacting olefin. Nevertheless, the TON for these substrates are still respectable. The nitrato-complexes **6.24–6.27** showed almost no significant differences in either conversion or Z-selectivity for the substrates where they were compared head-to-head. Finally, the selectivity for the Z-olefin was excellent in almost every case.

Having established the effectiveness of **6.24** in several homodimerizations reactions, we turned our attention to more complex reactions including the “standard” cross-metathesis reaction between **6.3** and *cis*-1,4-diacetoxycyclohexene

(**6.4**).²¹ Similar to the case of olefin homodimerization, lowering the temperature and increasing the substrate concentration resulted in higher conversion to the desired product (**6.5**) with comparable selectivity for the Z-olefin (Table 6.9). For this assay, all of the carboxylate catalysts performed roughly the same, reaching around 15 TON. Significant amounts of **6.6** were also formed in each reaction. In contrast, **6.24** was able to achieve similar levels of conversion at catalyst loadings as low as 1 mol%. Furthermore, since **6.4** possibly interferes with **6.24**, as evidenced by the low yields achieved in the homodimerization of **6.8**, we suspect that a judicious choice of substrates will allow for the catalyst loading to be lowered even further.

As mentioned above, we have previously established that the adamantyl group in catalysts such as **6.2** is critical for achieving high levels of Z-selectivity.⁶ The results presented above clearly demonstrate that the other X-type ligand plays an important role in reactivity, stability, and selectivity as well. The best demonstration of the significance of this ligand is the observed difference in initiation rates, where catalysts containing monodentate ligands (**6.18** and **6.23**) were essentially unreactive. This result implies that bidentate ligands are unique in their ability to induce catalyst initiation. Although ruthenium catalysts containing carboxylate²² or nitrato²³ ligands are well known, to the best of our knowledge, there has been no report on their initiation behavior, at least for catalysts with chelated oxygen ligands. However, analogues of **6.A** containing carboxylate or other bidentate ligands are generally metathesis active,²⁴ which is a certain indication that special ligands are not required for standard catalysts to initiate. It is also worth noting that the

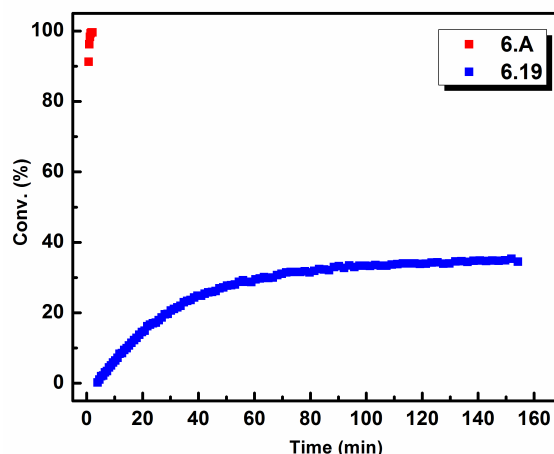


Figure 6.17. ROMP comparison of COD (**6.35**) with catalysts **6.A** and **6.19** (0.1 mol%) and **6.35** (53 μ L, 0.4 mmol), C_6D_6 (0.8 mL)

replacement of chlorides or carboxylates with nitrate in other ruthenium complexes generally resulted in less active and less selective metathesis catalysts.^{22,23} Thus, the C-H-activated catalysts appear to be unique in this regard.

A more general understanding of catalyst initiation can be gained by considering the differences in rates between complexes within the same family (e.g., carboxylates). For instance, electron-withdrawing and bulky groups resulted in an increase in initiation rate while smaller groups lead to a decrease in rate. Considering these results, it would have been interesting to probe the effect of electron-withdrawing carboxylates (e.g., trifluoroacetate). However, we discovered that such complexes were unstable and immediately decomposed upon anion exchange (Figure 6.14). Overall, the differences in initiation rates between catalysts with different carboxylates imply that a simple associative or associative-interchange mechanism is not occurring and that catalysts such as **6.2** likely undergo multiple pre-equilibrium steps (e.g., an equilibrium between κ^2 and κ^1 coordination, and an

equilibrium between association and dissociation of the chelated oxygen) prior to reaction with olefin.

Unfortunately, while our initiation rate studies allowed us to identify poor or unreactive catalysts (e.g., with monodentate ligands), they did not correlate with actual metathesis reactivity. Consider, for instance, the negligible difference in initiation rate between **6.A** and **6.19**. From this result, we predicted that these two complexes might have similar reactivity. A time-course plot for the conversion of cyclooctadiene (COD, **6.35**) during ring-opening metathesis polymerization (ROMP) revealed that this is clearly not the case (Figure 6.17). Catalyst **6.A** is able to complete this reaction within minutes, while **6.19** only reacts over a period of hours and never reaches full conversion. Furthermore, when compared with **6.2** and **6.24**, **6.19** is clearly inferior in terms of both activity and selectivity.

Therefore, simply increasing the initiation rate of the C-H-activated catalysts will not necessarily result in increased activity. On the other hand, decreasing the initiation rate does not result in an improved catalyst either. In the extreme case, this was shown by the inactivity of monodentate ligands, but it was also demonstrated by the lower activity of **6.20**. These observations parallel the behavior of previous generations of ruthenium metathesis catalysts.⁸ Although a complete mechanistic understanding of initiation for C-H-activated catalysts currently remains out of reach, the observed discrepancies between initiation rates and actual metathesis activity can most likely be explained by the fact that the method used to measure initiation does not take into account catalyst stability, the reversibility of metathesis reactions, or degenerate metathesis events (see Chapter 4). All of these factors

likely have a significant effect on the measured activity of the C-H-activated catalysts, particularly in cross-metathesis reactions.

In contrast to the various carboxylate ligands, changes to the aryl group on the NHC had little to no effect on catalyst initiation and activity. One exception was the replacement of mesityl (**6.24**) with 2,6-dimethyl-4-chlorobenzene (**6.27**), which resulted in a slight attenuation of initiation rate. Nonetheless, this only slightly affected catalytic activity as evidenced by the small differences in turnover frequency (TOF) between **6.24** and **6.27**. As mentioned earlier, we have been unable to access aryl groups significantly different from mesityl due to decomposition upon attempted C-H activation. For instance, we have demonstrated that ortho substitution of the aryl ring is required to prevent undesired C-H activation and subsequent decomposition.¹⁶ The remote nature of this part of the NHC ligand makes the predictability of structural effects on catalyst activity and selectivity difficult,²⁵ while the unpredictability associated with the synthesis of C-H-activated catalysts with different N-Aryl groups renders these modifications less convenient for catalyst optimization.

In actual cross-metathesis reactions, the nitrato catalysts **6.24–6.27** were the best catalysts in terms of both activity and selectivity. At this time, we believe this is a result of the nitrato ligand imparting greater stability to the complex compared with carboxylates. Qualitatively, **6.24–6.27** were far more tolerant to O₂ than the carboxylate analogues and also easier to purify. For instance, when a solution of **6.24** in C₆D₆ was exposed to air, the benzylidene resonance of **6.24** was still observed by ¹H NMR spectroscopy after 12 h. In contrast, the benzylidene

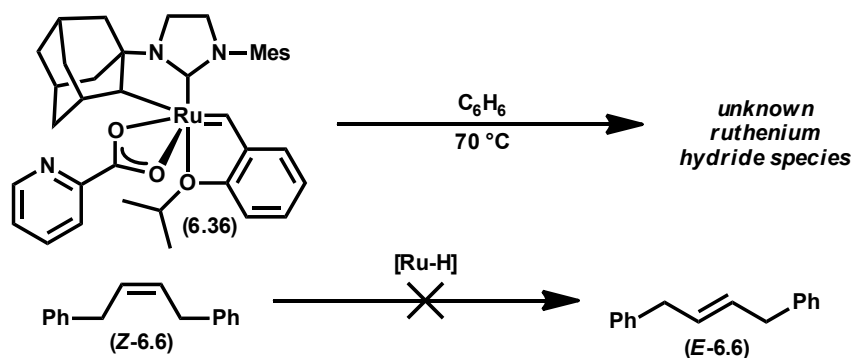


Figure 6.18. Generation of stable Ru hydrides [Ru-H] and attempted isomerization reaction

resonance of **6.2** disappeared after only 2 h following exposure to air. The reasons for this enhanced stability are unclear at this time, but there are clearly substantial steric and electronic effects at play. Thus, the effect of various bidentate and monodentate ligands on C-H-activated ruthenium catalysts will continue to be a focus of our research.

As with Mo- and W-based catalysts, the relationship between conversion and *Z*-selectivity is critical and warrants further discussion.³ At low reaction conversions, **6.24** is almost perfectly selective for the *Z*-olefin. Unfortunately, as conversion increases, *Z*-selectivity decreases at a rate dependent on the nature of the substrate, although it typically stays above 70%. This decrease in selectivity may be due to secondary metathesis events or to hydride-induced olefin isomerization.²⁶ A secondary metathesis mechanism would require the generation of a nonselective metathesis active decomposition product, since the initial catalyst is very selective. Several possible structures can be envisioned, the most likely of which would be a catalyst resulting from cleavage of the Ru-C (adamantyl) bond. Thus far, we have been unable to detect or isolate any species which may be

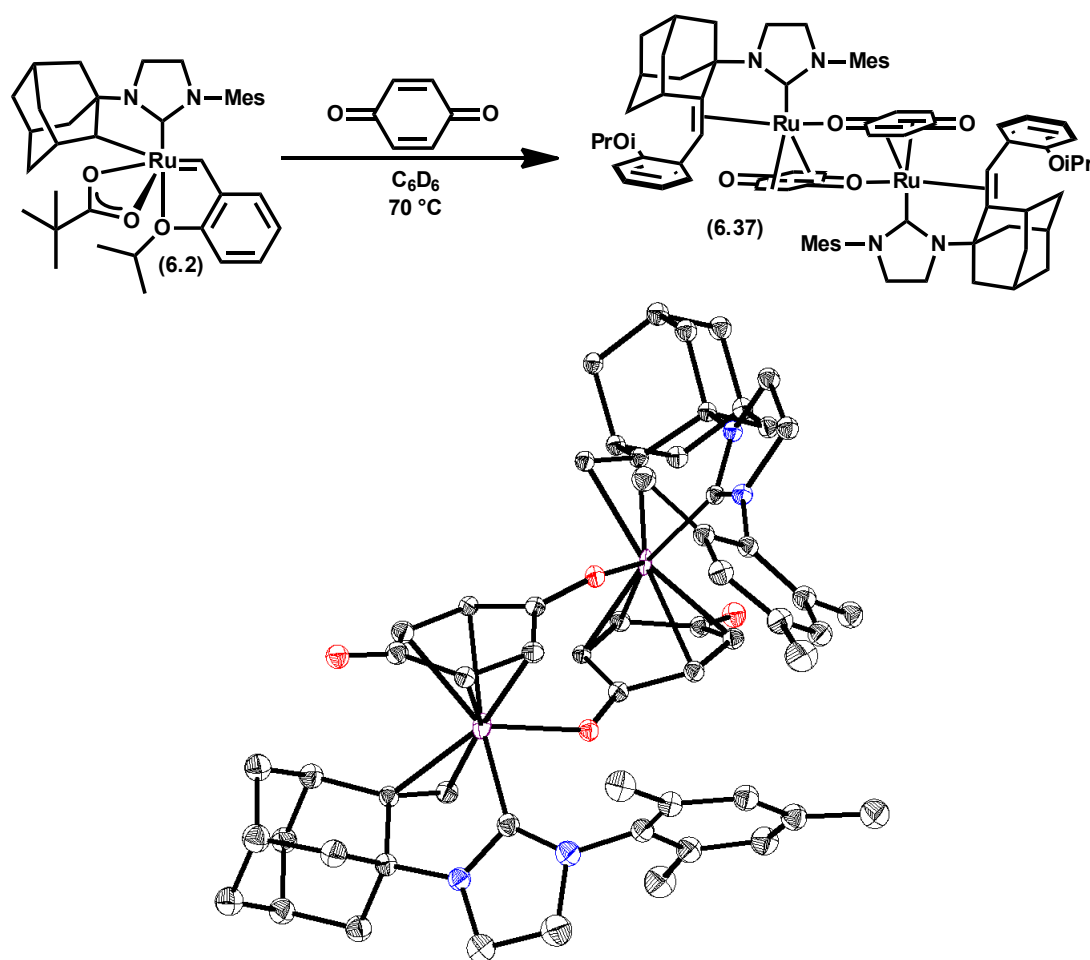


Figure 6.19. Benzoquinone-induced decomposition of **6.2** and solid-state structure of **6.37** drawn with 50% ellipsoids. Phenyl isopropoxy groups admitted for clarity

responsible for secondary metathesis. On the other hand, the existence of ruthenium hydrides can be inferred by the observation of olefin migration in the reaction of **6.3**. Moreover, these species can also be detected by ^1H NMR spectroscopy under special conditions. For example, when **6.18** was reacted with silver picolinate, the desired complex **6.36** was formed. However, **6.32** proved to be thermally unstable and spontaneously decomposed into a mixture of stable Ru hydride species that were detectable by ^1H NMR spectroscopy (Figure 6.18). When this mixture was exposed to a sample of *Z*-**6.6**, very little *Z* to *E* isomerization was

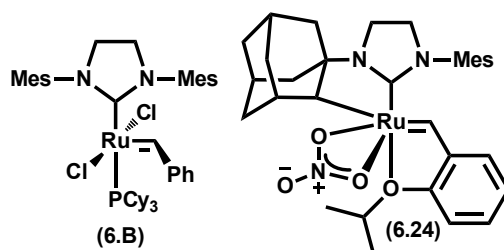


Figure 6.20. Catalysts examined for stereoselective ROMP

observed, suggesting that Ru-H species are not responsible for the degradation in Z-selectivity with certain substrates. Nevertheless, the identification of the species responsible for olefin isomerization (from *Z* to *E*) will be critical in establishing design parameters for future generations of Z-selective catalysts.

We have attempted to suppress the generation of hydride species and other deleterious decomposition products with various chemical quenchers, but have had little luck so far.²⁷ For example, benzoquinone has been shown to reduce olefin isomerization in cross-metathesis reactions. Unfortunately, **6.2** immediately decomposed in the presence of benzoquinone to give the crystallographically characterized dimer **6.37** (Figure 6.19). Other additives such as α,α -dichlorotoluene and chloroform yielded similar results. As a consequence of these results, the design of new catalysts that are less susceptible to either secondary metathesis or hydride formation is of paramount importance. For now, individual researchers must prioritize either conversion or Z-selectivity with substrates that are more susceptible to isomerization (i.e., alcohols).

Having prepared a robust Z-selective catalyst (**6.24**) that excelled at Z-selective cross-metathesis, we turned our attention to other potential metathesis applications, namely Z-selective ROMP. ROMP has long been used as a method

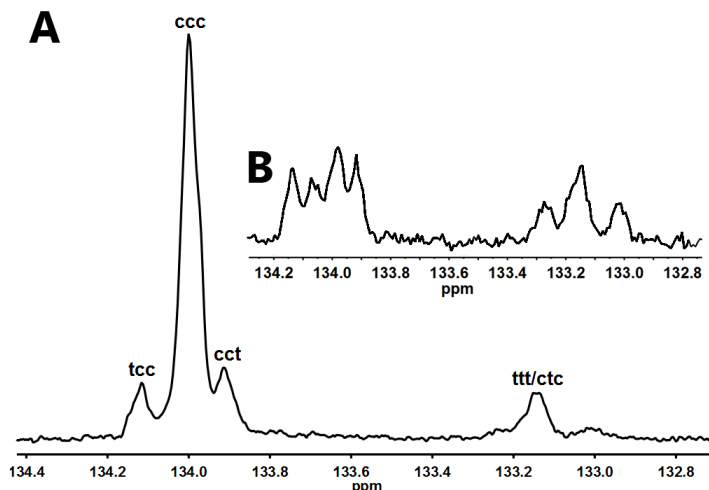


Figure 6.21. (A) ^{13}C NMR spectrum (CDCl_3) of **poly-6.38** prepared from **6.24** (0.5 mmol) and **6.24** (0.005 mmol) in THF (2 mL) at RT. “ccc” and “cct” represent cis-cis-cis cis-cis-trans triads consistent with literature reports.² (B) ^{13}C NMR spectrum of **poly-6.38** prepared from **6.24**

for preparing polymers with specific microstructures comprising various tacticities (e.g., atactic, isotactic, syndiotactic), double-bond geometries (cis/trans), and relative monomer configurations (e.g., head-to-tail, head-to-head, etc.).² Control of these microstructures is essential for preparing polymers with well-defined properties. Several metathesis catalysts based on Re, Os, Mo, and W have demonstrated impressive control over polymer microstructure, including high cis content (% cis) and well-defined tacticities.^{28,29} In contrast, Ru-based initiators such as $(\text{PCy}_3)_2\text{Cl}_2\text{Ru}=\text{CHPh}$ give almost exclusively trans polymer and yield tactic polymers only under very special circumstances.^{30,31,32} Indeed, this has been a serious limitation for previous generations of Ru-based metathesis catalysts, as recently highlighted by Schrock and co-workers.²⁸ The best literature examples of stereoselective ROMP with Ru catalysts including alternating copolymerization of norbornene and cyclo-alkenes to give polymers with 50–60% cis double bonds

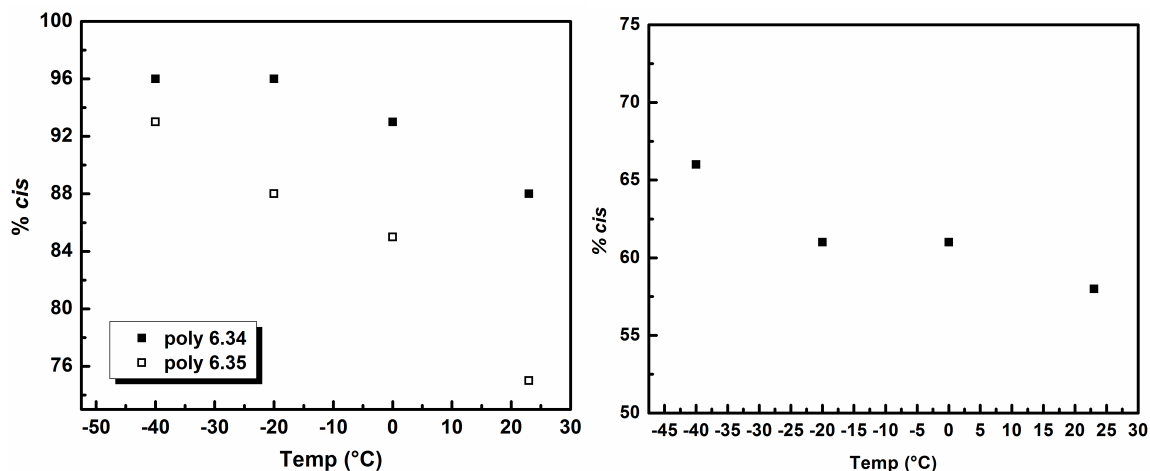
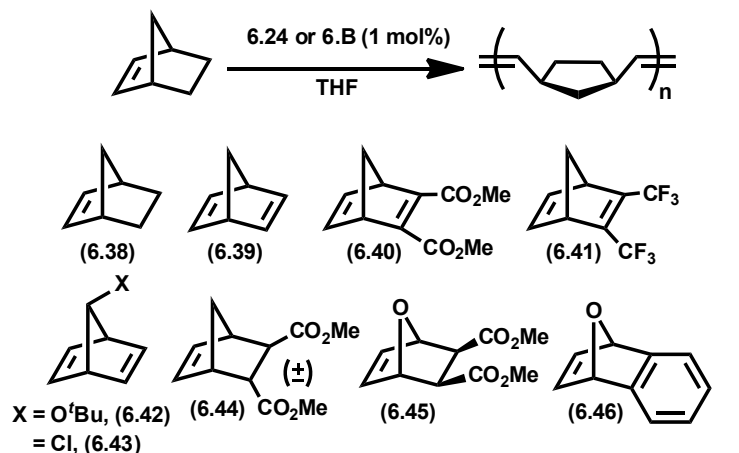


Figure 6.22. (left) change in % *cis* with temperature for **poly-6.38** and **poly-6.39** polymerized with **6.24**. Conditions were monomer (0.5 mmol) and **6.24** (0.005 mmol) in THF (2 mL). *Cis* content was determined by ^1H NMR spectroscopy. (right) Temperature dependence of % *cis* of **poly-6.38** prepared from **6.B**. Conditions were monomer (0.5 mmol) and **6.B** (0.005 mmol) in THF (2 mL). *Cis* content was determined by ^1H NMR spectroscopy. For temperatures 0 °C, –20 °C, and –40 °C, $(\text{H}_2\text{IMes})\text{Cl}_2\text{Ru}(\text{=CH-}o\text{-iPr-Ph})$ (**6.A**) was used as the catalyst.

and more recently up to 75%.^{33,34} Our group has described similar % *cis* values for sulfonate and phosphate substituted NHC-based catalysts as well.³⁵ In light of these results, we decided to examine the performance and selectivity of our *Z*-selective catalyst **6.24** in the context of ROMP.

When **6.24** was added to a solution of norbornene (**6.38**) in THF at room temperature (RT), an immediate increase in the viscosity of the solution occurred. Isolation of the resulting polymer (**poly-6.38**) and subsequent characterization by ^1H and ^{13}C NMR spectroscopy revealed that it contained ca. 88% *cis* double bonds (Figure 6.21). In contrast, **poly-6.38** prepared using **6.B** showed % *cis* values of 58% (Table 6.10).³⁶ These later values are typical of NHC-supported Ru-based metathesis catalysts. Importantly, an even higher selectivity of ca. 96% *cis* could be obtained with **6.24** by lowering the temperature of the monomer solution prior

Table 6.10. Polymerization of **6.38–6.46** with catalysts **6.B** and **6.24**^a



Monomer	Catalyst	Cis, ^b %	Yield, ^c %	M _n , ^d kDa	PDI ^d
6.38	6.B	58	88	112	1.65
	6.24	88	94	347	1.87
6.39	6.B	< 5	93	— ^e	— ^e
	6.24	75	88	—	—
6.40	6.B	93	78	95.5	1.21
	6.24	86	91	—	—
6.41	6.B	78	95	179	1.24
	6.24	61	40	137	1.21
6.42	6.B	58	78	—	—
	6.24	84	73	—	—
6.43	6.B	50	64	144	1.08
	6.24	69	81	328	1.09
	6.24	80 ^f	79	—	—
6.44	6.B	81	95	484	1.49
	6.24	91	78	629	1.33
6.45	6.B	66	> 95	463	1.5
	6.24	74	93	183	1.2
	6.24	80 ^f	79	—	—
6.46	6.B	67	> 95	—	—
	6.24	76	47	—	—
	6.24	91 ^{f,g}	80	—	—

^a Conditions were monomer (1 mmol) and catalyst (0.01 mmol) in THF (4 mL, 0.025 M) at RT. ^b Determined by ¹H NMR and ¹³C NMR spectroscopy. ^c Isolated yield. ^d Determined by multiangle light scattering (MALS) gel permeation chromatography (GPC). ^e Here and below: not determined due to insolubility of the isolated polymer in THF or DMF. ^f Reaction performed at –20 °C. ^g 0.3 mol% catalyst was used.

to the addition of the catalyst. This trend was also observed when norbornadiene (**6.39**) was reacted with **6.24** at different temperatures (Figure 6.22). The almost

exclusive formation of *cis* **poly-6.39** with **6.24** is particularly noteworthy since **6.B** gave no detectable amount of the *cis* isomer. Lowering the temperature of polymerizations using **6.B** resulted in only a slight increase in % *cis* that was never more than 5%. In addition to temperature changes, solvent effects have been shown to increase *cis* content in certain situations.³⁰ However, in the case of **6.24**, no change in *cis* content (for **poly-6.38**) was observed when the reaction solvent was changed from THF to benzene, dioxane, or DME. Moreover, both **poly-6.38** and **poly-6.39** prepared with **6.24** were atactic, as evidenced by the lack of peaks in the ¹³C NMR spectrum corresponding to either isotactic or syndiotactic polymer.

Having established that **6.24** could furnish polymers with high *cis* content for both **6.38** and **6.39**, we turned our attention to more complex monomers. Many of these monomers have been polymerized with very high *cis* selectivity and tacticity control using Mo- and W-derived catalysts, but formed predominantly *trans* polymers when (PCy₃)₂Cl₂Ru=CHPh was used.³⁰ Gratifyingly, we found that in almost every case, **6.24** yielded a polymer with high *cis* content approaching 90%. In the cases where *cis*-selectivity with **2** at RT was below that value, conducting ROMP at –20 °C increased % *cis* by 6–15% (Table 6.10). In general a lower fraction of *cis* double bonds was observed for polymers prepared using **6.B**. However, in the case of monomers **6.40**, **6.41**, and **6.42**, high *cis* content was achieved without the use of a specially designed catalyst! This is particularly surprising since the closely related (PCy₃)₂Cl₂Ru=CHPh is known to give **poly-6.40** with only 11% *cis* double bonds.³⁰ In contrast to **poly-6.40** and **poly-6.44** prepared by Mo-based

Table 6.11. Polymerization of **6.35**, **6.47**, and **6.49** with catalysts **6.B** and **6.24**^a

Monomer	Catalyst	Time(h)	Cis, ^b %	Yield, ^c %	M _n , ^d kDa	PDI ^d
cyclooctadiene (6.35)	6.B	1	10	88	22.9	1.64
	6.24	36	96	19	99.1	1.60
cyclopentene (6.47)	6.B	5	15	68	11.1	1.47
	6.24	3	48	24	102	1.40
<i>trans</i> -cyclooctene (6.49)	6.B	1	18	49	— ^e	—
	6.24	1	70	44	—	—

^a See experimental section for reaction conditions. ^b cis content of polymer determined by ¹H NMR and ¹³C NMR spectroscopy. ^c Isolated yield. ^d Determined by MALS GPC. ^e Not determined due to insolubility of the isolated polymer in THF or DMF

catalysts,²⁹ no long-range order was observed using either of the Ru-based initiators. With **6.24**, the formation of atactic polymers can be explained by fast carbene epimerization relative to the rate of propagation or an inherent lack of facial selectivity. As mentioned above, this result is typical of Ru-based catalysts.

Experimental molecular weights (M_n) for polymers prepared with **6.24** were generally higher than the predicted values, which is indicative of incomplete catalyst initiation or a high rate of propagation (k_p) relative to the rate of initiation (k_i). This could be qualitatively observed as a solution of **6.24** and **6.34** remained purple (the color of **6.24**), even after complete conversion of the monomer. Based on the relatively low initiation rate constant of **6.24**, this result was expected.³⁷

In contrast to norbornene and norbornadiene-type monomers, cyclooctadiene (COD, **6.35**), cyclopentene (**6.47**), and *cis*-cyclooctene (**6.48**) are significantly more difficult to polymerize via ROMP due to their lower ring-strain.³⁸ Furthermore, the Z-selective ROMP of these monomers is particularly challenging due to the prevalence of intra- and intermolecular chain-transfer reactions and secondary metathesis events.³⁹ In fact, the Z-selective ROMP of **6.31** has only

recently been reported using a Mo metathesis catalyst.^{29,40} Given the strong preference of **6.24** for *cis*-selective polymerization of bicyclic monomers, the next logical step was to attempt the ROMP of more difficult substrates, such as **6.35**, **6.47**, and **6.48**.

When **6.35** was exposed to **6.24** (1 mol%) in C₆D₆ (0.6 mL), only minimal conversion (< 20%) was observed after 24 h at RT. Surprisingly, increasing the temperature did not result in higher conversions, despite the fact that no catalyst decomposition was observed by ¹H NMR spectroscopy. Increasing the substrate concentration and switching the solvent to THF also did not increase the conversion of **6.35**, nor did repeating the reaction in neat **6.35**. However, polymerizing **6.35** with **6.24** in THF at RT over a period of 3 days provided a modest amount of **poly-6.35** (19% yield). Isolation and subsequent analysis of **poly-6.35** via ¹³C NMR spectroscopy revealed that it contained 96% *cis* double bonds, a value comparable to that obtained with the Mo-based system (Table 6.11). Similar to the ROMP of **6.38** (norbornene) and **6.39** (norbornadiene), increasing the temperature of the polymerization of **6.35** resulted in polymers with lower *cis* content, although it never went below 80%. The extraordinariness of the above result is highlighted by the fact that **6.B** yielded **poly-6.35** with 90% *trans* selectivity (Table 6.11).³⁷

Subsequent to our experiments with **6.35**, we found that **6.24** was also effective at polymerizing **6.47**, although the isolated yield of **poly-6.47** was still low (Table 6.11). Characterization of **poly-6.47** by ¹³C NMR spectroscopy revealed 48% *cis* content, which is significantly lower than the *cis* content of **poly-6.35** prepared by **6.24**. Similar levels of *cis* selectivity have been reported in

copolymerizations with **6.47**, although these generally resulted from incomplete incorporation of **6.47**.^{33d} Switching to catalyst **6.B** produced **poly-6.47** with only 15% *cis* double bonds. Thus, the use of **6.24** resulted in a significant improvement in the *cis* content of **poly-6.47**, albeit to a lesser extent than was anticipated.

Unfortunately, no conversion of **6.48** was observed when it was exposed to **6.24** under a variety of conditions.⁴¹ This was surprising since the strain energy of **6.48** (7.4 kcal/mol) is greater than that of **6.47** (6.8 kcal/mol).³⁸ At this time, we believe that the steric size of **6.48** prevented its polymerization. Nevertheless, we reasoned that a more significant increase in strain energy, resulting from the use of *trans*-cyclooctene (**6.49**), would provide access to the desired polymer.⁴² Indeed, reaction of **6.24** with **6.49** at RT in THF resulted in the immediate and high yielding production of **poly-6.49**. Characterization of this polymer revealed a *cis* content of 70%, a value that is among the highest reported for ruthenium-based catalysts.⁴³ Notably, **poly-6.49** prepared from **6.B** contained ca. 82% *trans* double bonds.

As mentioned above, secondary metathesis events are common in non-rigid polymers, because the active chain end is capable of intra – (“back-biting”) and intermolecular chain transfer reactions. Taking this into account, the *cis* selective polymerizations of **6.35**, **6.47**, and **6.49** with **6.24** are remarkable. Indeed, given the very high % *cis* of **poly-6.35** and no erosion of *cis* content over the course of polymerization, one should conclude that **6.24** is less prone to isomerizing or reacting with internal double bonds in polymers while displaying high kinetic selectivity for the formation of *cis* double bonds. Our molecular weight data also supports this argument, as **poly-6.35/6.47** prepared from **6.24** had much higher

molecular weights compared to **poly-6.35/6.47** prepared from **6.B**. Such a result is consistent with a reduction in the number of chain transfer events, which tend to lower molecular weight.⁴⁴ The importance of controlling secondary metathesis is reinforced by examination of the polymers prepared from **6.B**. In the case of **poly-6.40/6.41/6.44**, where secondary metathesis is suppressed due to steric effects, catalyst **6.B** yielded polymers with relatively high *cis* content. In contrast, **poly-6.35/6.47** have no protection against secondary metathesis and thus the thermodynamically favored *trans* olefin is eventually formed when these polymers are prepared from **6.B**. Although we have not specifically investigated the mechanistic origin of Z-selectivity in ROMP, calculations performed on an analogue of **6.24** indicate that steric pressure exerted by the NHC on side-bound ruthenacycles is responsible for the observed Z-selectivity during cross-metathesis.^{33c,19} It is likely that a similar mechanism is also responsible for the selectivities observed above.

Conclusions and Future Outlook

In summary, we have prepared a variety of new C-H-activated ruthenium catalysts for Z-selective olefin metathesis. Adjusting the ligand environment around the metal center has yielded significant insight into the initiation behavior, activity, and selectivity of this class of catalysts and has facilitated the development of improved catalysts (**6.24–6.27**) that are capable of ca. 1000 TONs in several cross-metathesis reactions. We note that these catalysts can be used with very low loadings, and do not require reduced pressures, high temperatures, or rigorous exclusion of protic solvents in order to operate

effectively. Secondary metathesis events are also relatively slow for the majority of substrates, meaning that significant reaction optimization should not be required.

Furthermore, we also demonstrated the *cis* selective ROMP of several monomers using Ru-based catalysts. The resulting polymers were recovered in moderate to high yield and *cis* content ranged from 48–96%. While the *cis* content varied significantly based on monomer structure, our C-H activated catalyst (**6.24**) gave polymers with significantly higher % *cis* values compared to those prepared by a more traditional Ru metathesis catalyst (**6.B**), while also showing qualitatively reverse stereoselectivity compared to $(\text{PCy}_3)_2\text{Cl}_2\text{Ru}=\text{CHPh}$. These results culminated in the highly *cis* selective polymerization of **6.35**, thereby proving that *cis* selective ROMP is possible with Ru catalysts, even with monomers that are prone to secondary metathesis. Future work in our laboratory will focus on improvements to both the activity and *cis* selectivity of **6.24**, with an emphasis on the application of this exciting new class of catalysts towards the development of novel polymer architectures.

Based on these results, we anticipate that catalysts such as **6.24** will be swiftly adopted by both industrial and academic researchers interested in the construction of Z-olefins using metathesis methodology. Nevertheless, there is still room for improvement in both catalyst activity and selectivity.

Experimental

General: All reactions were carried out in dry glassware under an argon atmosphere using standard Schlenk line techniques or in a Vacuum Atmospheres Glovebox under a nitrogen atmosphere unless otherwise specified. All solvents

were purified by passage through solvent purification columns and further degassed with argon.⁴⁵ NMR solvents for air-sensitive compounds were dried over CaH_2 and vacuum transferred or distilled into a dry Schlenk flask and subsequently degassed with argon. Commercially available reagents were used as received unless otherwise noted. Substrates for olefin cross-metathesis (**6.3**, **6.7**, **6.8–6.17**) were degassed with argon and passed through a plug of neutral alumina (Brockmann I) prior to use.

Standard NMR spectroscopy experiments were conducted on a Varian Inova 400 MHz spectrometer, while kinetic experiments were conducted on a Varian 500 MHz spectrometer equipped with an AutoX probe. Experiments and pulse sequences from Varian's Chempack 4 software were used. Chemical shifts are reported in ppm downfield from Me_4Si by using the residual solvent peak as an internal standard. Spectra were analyzed and processed using MestReNova Ver. 7.

Gas chromatography data was obtained using an Agilent 6850 FID gas chromatograph equipped with a DB-Wax Polyethylene Glycol capillary column (J&W Scientific). High-resolution mass spectrometry (HRMS) data was obtained on a JEOL MSRoute mass spectrometer using FAB+ ionization, except where specified.

Polymer molecular weights were determined by multi-angle light scattering (MALS) gel permeation chromatography (GPC) using a miniDAWN TREOS light scattering detector, a Viscostar viscometer, and an OptilabRex refractive index detector, all from Wyatt Technology. An Agilent 1200 UV-Vis detector was also present in the detector stack. Absolute molecular weights were determined using dn/dc values calculated by assuming 100% mass recovery of the polymer sample injected into the GPC. No internal standards were used

Improved Synthesis of 6.2: In a glovebox, a 500 mL Schlenk flask was charged with **6.1** (0.98 g, 1.52 mmol), sodium pivalate (1.89 g, 15.2 mmol), THF (12 mL), and MeOH (12 mL). The flask was sealed, removed from the glove box and heated to 40 °C overnight (16 h) at which point the solution had changed color from green to brown to deep purple. The solvent was removed under high vacuum and the Schlenk flask was transferred back into the glove box where the residue was dissolved in CH₂Cl₂ (~ 150 mL), filtered through celite, and concentrated to a deep purple residue consisting of a mixture of the C-H-activated product and pivalic acid. Cold Et₂O was added to this residue and the resulting bright purple solid was collected by filtration. An additional crop of **6.2** was recovered by cooling the Et₂O washes from above to –35 °C and collecting the purple crystals that formed. Total yield was 0.62 mg of **6.2** (61% yield). NMR parameters were consistent with previous reports.⁶

Preparation of 6.18: In a glovebox, a 250 mL RB flask was charged with **6.2** (491 mg, 0.731 mmol), NaI (548 mg, 3.65 mmol), and THF (25 mL). The resulting suspension was stirred for 1 h, at which point a color change from purple to brown had occurred. The solution was concentrated and the residue was dissolved in CH₂Cl₂ (ca. 100 mL), filtered through celite, and concentrated to a brown residue which was triturated with Et₂O until the washes were colorless to give **3** (332 mg, 65%) as a brown solid. ¹H NMR (400 MHz, C₆D₆) δ 13.42 (s, 1H), 7.38 (dd, *J* = 8, 4 Hz, 1H), 7.15 (m, 1H), 6.97 (br s, 1H), 6.80 (dt, *J* = 8, 1 Hz, 1H), 6.76 (br s, 1H), 6.64 (d, *J* = 8 Hz, 1H), 4.81 (sept, *J* = 4 Hz, 1H), 3.46 (q, *J* = 8 Hz, 1H), 3.37–3.30 (m, 1H), 3.11–3.06 (m, 2H), 2.61 (br s, 1H), 2.56 (s, 3H), 2.41 (s, 3H), 2.40 (br s,

1H), 2.13 (s, 3H), 2.03 (br s, 1H), 1.91 (d, $J = 4$ Hz, 3H), 1.86–1.79 (m, 2H), 1.65 (br s, 2H), 1.62 (d, $J = 4$ Hz, 3H), 1.59–1.57 (m, 1H), 1.43–1.37 (m, 3H), 2.30 (br d, $J = 8$ Hz, 2H), 0.54 (br d, $J = 16$ Hz, 1H). ^{13}C NMR (126 MHz, C_6D_6) δ 236.56, 215.48, 154.59, 141.54, 139.13, 138.09, 137.45, 135.36, 125.96, 123.47, 122.63, 112.99, 81.52, 75.78, 63.40, 52.52, 42.24, 41.09, 39.39, 38.12, 37.54, 37.25, 33.81, 30.63, 29.64, 22.72, 21.76, 21.16, 20.99, 19.28. HRMS (FAB+): Calculated—698.1316, Found—698.1343.

Preparation of silver(I) 2,2-dicyclohexylacetate (6.19-Ag): To 2,2-dicyclohexylcarboxylic acid (1.24 g, 5.54 mmol) and NaOH (193 mg, 4.82 mmol) was added H_2O (2.7 mL) and the solution was stirred for 15 min. AgNO_3 (676 mg, 3.99 mmol) dissolved in H_2O (2.6 mL) was added drop-wise, which caused immediate precipitation of a white solid. The suspension was stirred for 15 min after which the white precipitate was collected on a medium porosity frit and washed with H_2O , MeOH, and hexanes. After drying, **4-Ag** was recovered as a white solid (937 mg, 71%). Insolubility precluded analysis using NMR spectroscopy. MS (laser desorption ionization): Calculated—223.1704, Found—223.1788.

Preparation of 6.19: In a glovebox, a 20 mL scintillation vial was charged with **6.18** (24 mg, 0.035 mmol) and **6.19-Ag** (13 mg, 0.038 mmol). THF (ca. 1 mL) was added and the color of the solution immediately changed from brown to deep purple. The reaction was stirred for 1 h and concentrated. The resulting purple residue was dissolved in C_6H_6 , filtered through celite, and concentrated to give **6.19** (25 mg, 93%).

Note: Catalyst **6.19** would change colors from purple to brown upon the addition of solvents which were not rigorously purified of oxygen. Recrystallization from Et₂O at –35°C was used to purify **6.19** when this occurred. ¹H NMR (400 MHz, C₆D₆) δ 14.94 (s, 1H), 7.41 (dd, *J* = 8, 4 Hz, 1H), 7.25 (dt, *J* = 8, 4 Hz, 1H), 6.87–6.83 (m, 2H), 6.80 (br s, 1H), 6.72 (br d, *J* = 8 Hz, 1H), 4.78 (sept, *J* = 8 Hz, 1H), 4.08 (s, 1H), 3.45–3.13 (m, 4H), 2.47 (br s, 1H), 2.44 (s, 3H), 2.33 (s, 1H), 2.25 (s, 1H), 2.10–1.30 (m, 10H), 2.07 (br s, 1H), 1.98 (br d, *J* = 8 Hz, 3H), 1.88 (br d, *J* = 8 Hz, 4H), 1.79 (br s, 3H), 1.76 (br s, 2H), 1.64 (br s, 4H), 1.60 (d, *J* = 4 Hz, 4H), 3.34 (br d, *J* = 16 Hz, 3H), 1.39 (br s, 1H), 1.36 (d, *J* = 4 Hz, 5H), 1.17 (br d, *J* = 8 Hz, 2H), 1.07 (br d, *J* = 8 Hz, 2H), 0.63 (br d, *J* = 12 Hz, 1H). ¹³C NMR (101 MHz, C₆D₆) δ 258.83, 214.74, 183.61, 153.90, 143.52, 137.70, 136.58, 136.43, 136.03, 129.47, 129.20, 124.98, 122.86, 122.83, 113.34, 73.83, 67.67, 62.30, 57.15, 51.31, 42.77, 40.96, 40.04, 37.88, 37.58, 36.76, 33.30, 30.71, 29.60, 21.68, 21.35, 20.86, 18.65, 18.49. HRMS (FAB+, (M+H)–H₂): Calculated—793.3883, Found—793.3894.

Preparation of 6.20: Catalyst **6.20** (23 mg, 80%) was prepared in a manner analogous to catalyst **6.19**. **6.18** (32 mg, 0.046 mmol), AgOAc (11 mg, 0.069 mmol), THF (ca. 1 mL). ¹H NMR (400 MHz, C₆D₆) δ 14.95 (s, 1H), 7.47 (dd, *J* = 7.6, 1.6 Hz, 1H), 7.25 (t, *J* = 7.2 Hz, 1H), 6.88 (dt, *J* = 7.6, 1.2 Hz, 1H), 6.77 (br s, 1H), 6.70 (br s, 1H), 6.65 (br d, *J* = 8.4 Hz, 1H), 4.76 (sept, *J* = 6.0 Hz, 1H), 4.06 (s, 1H), 3.47 (q, *J* = 8.8 Hz, 1H), 3.38–3.21 (m, 4H), 2.43 (s, 3H), 2.40 (br s, 1H), 2.33 (s, 3H), 2.15 (br s, 4H), 2.15–1.04 (m, 2H), 1.98–1.95 (m, 1H), 1.87–1.83 (m, 1H), 1.78 (s, 3H), 1.69 (br s, 1H), 1.57 (d, *J* = 6.4 Hz, 3H), 1.56–1.53 (m, 2H), 1.22–1.15 (m, 2H), 1.05 (d, *J* = 6.4 Hz, 3H), 0.73 (br d, *J* = 12 Hz, 1H). ¹³C NMR (101 MHz,

C₆D₆) δ 259.69, 215.65, 180.15, 154.57, 143.79, 137.76, 137.41, 136.81, 136.42, 129.55, 129.24, 125.51, 123.20, 123.19, 112.90, 74.01, 68.79, 67.84, 62.82, 51.44, 43.38, 41.62, 40.64, 38.27, 37.97, 37.72, 33.59, 31.21, 30.03, 25.84, 24.43, 21.35, 21.04, 20.73, 18.75, 18.48. HRMS (FAB+, (M+H)–H₂): Calculated—629.2318, Found—629.2345.

Preparation of 6.21: Thioacetic acid (2.1 g, 28.2 mmol) was added to a solution of NaOH (1.2 g, 29.4 mmol) in 30 mL H₂O and stirred for 15 min at RT. A solution of AgNO₃ (3.9 g, 23.5 mmol) in 30 mL H₂O was added which resulted in an immediate color change and formation of a brown precipitate. The suspension was stirred for 15 min, after which the precipitate was collected by filtration and washed with H₂O, MeOH, and Et₂O to give **6.21-Ag** as a grey powder (2.49 g, 58% yield) which was used without further purification or characterization.

Catalyst **6.21** (16 mg, 77%) was prepared in a manner analogous to **6.19**. **6.18** (22 mg, 0.0312 mmol), **6.21-Ag** (18 mg, 0.101 mmol), and THF (1 mL). ¹H NMR (400 MHz, C₆D₆) δ 14.89 (s, 1H), 7.38 (dd, *J* = 7.2, 1.6 Hz, 1H), 7.19 (m, 1H), 6.81 (m, 2H), 6.77 (br s, 1H), 6.69 (d, *J* = 8.4 Hz, 1H), 4.81 (sept, *J* = 5.6 Hz, 1H), 4.03 (br s, 1H), 3.45 (m, 1H), 3.36 (m, 1H), 2.59 (s, 1H), 2.43 (s, 3H), 2.35 (m, 1H), 2.29 (s, 3H), 2.22 (s, 3H), 2.18 (br s, 1H), 2.08 (s, 3H), 1.93 (m, 2H), 1.93 (m, 1H), 1.73 (br s, 1H), 1.59 (br m, 3H), 1.49 (d, *J* = 6.4 Hz, 3H), 1.32 (d, *J* = 6 Hz, 4H), 1.25 (m, 3H), 0.76 (m, 1H). HRMS (FAB+, (M+H)–H₂): Calculated—645.2089, Found—645.2068.

Preparation of silver(I) 2,2-dimethoxypropanoate (6.22-Ag): A 100 mL RB flask was charged with 2,2-dimethoxypropanoic acid (488 mg, 3.64 mmol), Ag₂O (507

mg, 2.19 mmol), MeCN (20 mL), and H₂O (6 mL). The solution was shielded from light and stirred at RT under Ar for 5 h. The suspension was filtered through celite, washing with MeCN, and the filtrate was concentrated to a white solid which was washed with hexanes and collected by filtration to give **6.21-Ag** (469 mg, 53%). ¹H NMR (400 MHz, D₂O) δ 3.21 (s, 6H), 1.43 (s, 3H). ¹³C NMR (101 MHz, D₂O) δ 176.37, 101.51, 49.34, 20.26. MS (laser desorption ionization): Calculated—133.0506, Found—133.0539.

Preparation of 6.22: Catalyst **6.22** (31 mg, 89%) was prepared in a manner analogous to catalyst **6.19**. **6.18** (35 mg, 0.050 mmol), **6.22-Ag** (13 mg, 0.055 mmol), THF (ca. 1 mL). ¹H NMR (600 MHz, C₆D₆) δ 14.88 (s, 1H), 7.43 (br d, *J* = 12 Hz, 1H), 7.23 (t, *J* = 6 Hz, 1H), 6.94 (br s, 1H), 6.86 (t, *J* = 6 Hz, 1H), 6.74–6.71 (m, 2H), 4.87 (br s, 1H), 4.16 (s, 1H), 3.50–3.19 (m, 10H), 2.47 (br s, 1H), 2.45 (s, 3H), 2.40 (s, 3H), 2.20 (s, 3H), 2.13–2.08 (m, 2H), 2.01 (br d, *J* = 12 Hz, 1H), 1.96 (br d, *J* = 12 Hz, 1H), 1.82 (br d, *J* = 12 Hz, 1H), 1.66 (br s, 1H), 1.63 (d, *J* = 6 Hz, 3H), 1.57–1.54 (m, 1H), 1.50–1.48 (m, 1H), 1.43 (br d, *J* = 12 Hz, 1H), 1.38 (s, 3H), 1.27 (br d, *J* = 6 Hz, 3H), 1.17 (br d, *J* = 12 Hz, 1H), 1.10–1.09 (m, 2H), 0.68 (br d, *J* = 6 Hz, 1H). ¹³C NMR (151 MHz, C₆C₆) δ 259.06, 216.37, 177.95, 154.78, 144.04, 138.48, 137.86, 136.61, 136.38, 130.46, 129.48, 125.96, 123.52, 123.39, 113.89, 99.58, 75.37, 69.60, 63.10, 51.94, 43.58, 41.83, 40.83, 38.50, 38.32, 37.63, 33.94, 31.45, 30.30, 21.70, 21.41, 21.17, 20.99, 19.11, 18.88. HRMS (FAB+, (M+H)–H₂): Calculated—703.2685, Found—703.2682.

Preparation of 6.23: In a glove box, **6.2** (52.1 mg, 77.5 μmol), potassium 2,6-diisopropylphenoxide (83.9 mg, 388 μmol) and C₆H₆ (5.0 ml) were added into

a 20 ml vial equipped with a stir bar. The reaction mixture was stirred at room temperature for 30 min and filtered. The filtrate was evaporated and the resulting solid was dissolved in small amount of Et₂O and recrystallized at □35 °C. **11** was obtained as dark brown crystals (54 mg, 93%). ¹H NMR (500 MHz, C₆D₆): δ 14.02 (s, 1H), 7.39 (dd, *J* = 7.3, 1.5 Hz, 1H), 7.15 (br s, 1H), 7.06 (dt, *J* = 6.5, 2 Hz, 1H), 6.95 (br s, 1H), 6.83 (q, *J* = 7.5 Hz, 2H), 6.77 (s, 1H), 6.58–6.57 (m, 2H), 4.32 (sept, *J* = 6.4 Hz, 1H), 4.0 (br s, 1H), 3.89 (s, 1H), 3.40 (q, *J* = 11 Hz, 1H), 3.27 (dt, *J* = 10.5, 5 Hz, 1H), 3.10 (m, 2H), 2.57 (s, 3H), 2.33 (s, 3H), 2.30 (br s, 1H), 2.20 (br s, 1H), 2.11 (br s, 1H), 2.03 (s, 3H), 2.01 (br s, 1H), 1.94–1.93 (m, 1H), 1.82 (br t, *J* = 9 Hz, 2H), 1.62 (br s, 1H), 1.55–1.38 (m, 9H), 1.25 (d, *J* = 6.4 Hz, 3H), 1.11 (br d, *J* = 10.5 Hz, 2H), 0.85 (d, *J* = 6.4 Hz, 3H), 0.59–0.41 (br m, 7H). ¹³C NMR (126 MHz, C₆D₆) δ 234.91, 214.14, 150.56, 140.03, 136.31, 134.41, 134.07, 132.39, 127.15, 126.11, 121.95, 119.99, 119.76, 112.66, 110.58, 72.80, 66.00, 60.25, 49.43, 40.14, 38.44, 37.35, 34.95, 34.83, 34.23, 30.62, 27.99, 26.83, 18.48, 18.15, 17.71, 15.97, 15.73. HRMS (FAB+): Calculated—748.3542, Found—748.3576.

Preparation of 6.24: Method A: In a glovebox, a 20 mL scintillation vial was charged with **6.18** (112 mg, 0.161 mmol), AgNO₃ (409 mg, 2.41 mmol), and THF (6 mL). The reaction was stirred vigorously until a color change from brown to dark purple was observed (ca. 3–5 min). At this point, the reaction was immediately concentrated and the resulting residue was dissolved in C₆H₆, filtered, and concentrated. The crude product was triturated with Et₂O several times, until the washes were colorless, to give **7** (73 mg, 72%) as a purple solid. ¹H NMR (400 MHz, C₆D₆) δ 15.22 (s, 1H), 7.37 (d, *J* = 7.2 Hz, 1H), 7.18 (t, *J* = 7.6 Hz, 1H), 6.98

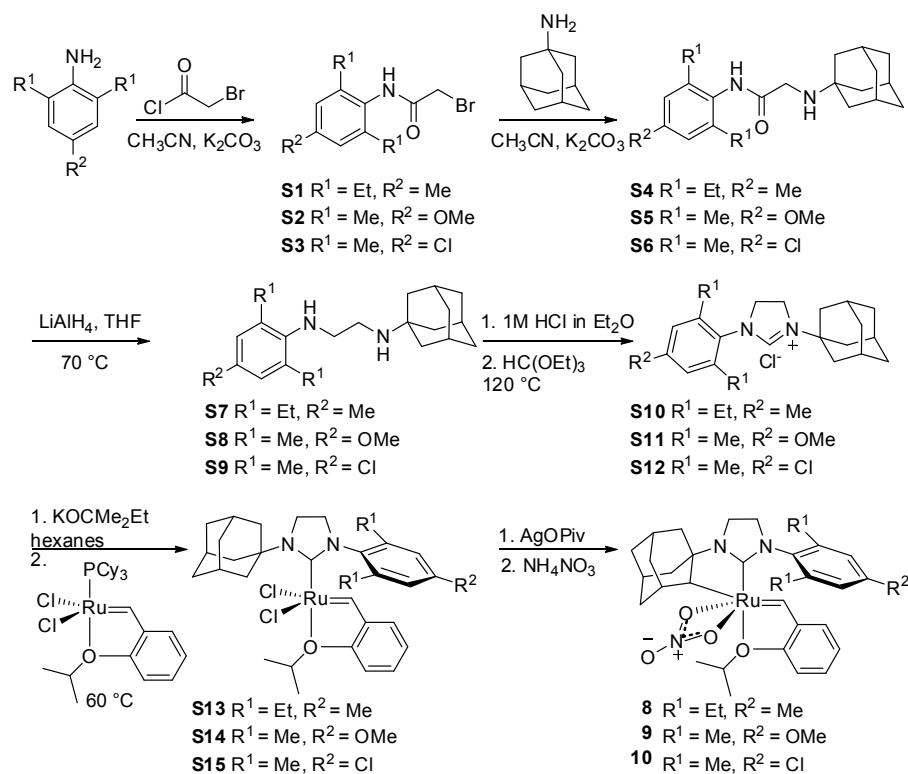


Figure 6.S1. Synthesis of catalysts **6.25**, **6.26**, **6.27**.

(s, 1H), 6.82 (t, $J = 7.6$ Hz, 1H), 6.66 (s, 1H), 6.48 (d, $J = 8.4$ Hz, 1H), 4.57 (sept, $J = 6.0$ Hz, 1H), 4.17 (s, 1H), 3.43 (q, $J = 9.6$ Hz, 1H), 3.28–3.15 (m, 3H), 2.38 (d, $J = 8.4$ Hz, 6H), 2.25 (br s, 1H), 2.15–2.09 (m, 4H), 2.03–1.97 (m, 2H), 1.90–1.87 (m, 1H), 1.77 (br d, $J = 15.2$ Hz, 1H), 1.65 (br s, 1H), 1.55–1.47 (m, 2H), 1.42 (d, $J = 5.2$ Hz, 3H), 1.14–1.10 (m, 3H), 0.96 (d, $J = 6.0$ Hz, 3H), 0.58 (br d, $J = 12$ Hz, 1H). ^{13}C NMR (101 MHz, C_6D_6) δ 265.80, 265.55, 214.16, 154.72, 143.60, 137.69, 137.40, 136.24, 135.45, 130.11, 129.36, 126.83, 123.38, 123.35, 113.00, 74.32, 66.78, 63.05, 51.36, 43.14, 41.84, 40.34, 37.95, 37.81, 37.65, 33.33, 30.98, 29.83, 21.25, 21.09, 20.28, 18.56, 17.44. HRMS (FAB+, $\text{M}-\text{NO}_3$): Calculated—571.2263, Found—571.2273.

Method B: In a glovebox, a 20 mL scintillation vial was charged with **6.2**

(128 mg, 0.190 mmol), NH_4NO_3 (457 mg, 5.71 mmol), and THF (ca. 10 mL). The reaction was stirred until completion as determined by ^1H NMR spectroscopy (ca. 1h) and concentrated. The residue was purified as described in Method A to give **6.24** (98 mg, 82%). Note: crude **6.2** as prepared above could also be used to prepare **6.24**.

Preparation of S1: A solution of 2,6-diethyl-4-methylaniline (1.63 g, 10.0 mmol) and CH_3CN (20 mL) was treated with K_2CO_3 (2.76 g, 20.0 mmol). Bromoacetyl chloride (830 μL , 10.0 mmol) was added drop-wise, and the reaction mixture was stirred at 25 $^\circ\text{C}$ over 12-16 h. The mixture was filtered over celite, concentrated under reduced pressure, and recrystallized from CH_2Cl_2 -hexanes providing S1 (1.55 g, 55%) as a white powder: ^1H NMR (CDCl_3 , 500 MHz) δ 7.68 (s, 1H), 6.95 (s, 2H), 4.08 (s, 2H), 2.54 (q, 4H, $J = 7.5$ Hz), 2.32 (s, 3H), 1.19 (t, 6H, $J = 7.5$ Hz); ^{13}C NMR (CDCl_3 , 125 MHz) δ 164.8, 141.2, 138.2, 129.1, 127.4, 29.2, 24.8, 21.3, 14.6; HRMS (FAB+) m/z : Calculated—([M + H]) 284.0650, Found—284.0654 ([M + H]).

Preparation of S2: Prepared from 4-methoxy-2,6-dimethylaniline⁴⁶ (520 mg, 3.44 mmol) and bromoacetyl chloride (286 μL , 3.44 mmol) following the procedure detailed for **S1** providing **S2** (750 mg, 80%) as a white powder: ^1H NMR (CDCl_3 , 500 MHz) δ 7.66 (s, 1H), 6.62 (s, 2H), 4.04 (s, 2H), 3.77 (s, 3H), 2.20 (s, 6H); ^{13}C NMR (CDCl_3 , 125 MHz) δ 164.5, 158.7, 136.9, 125.9, 113.6, 55.4, 29.2, 18.6; HRMS (EI+) m/z : Calculated—271.0208, Found—271.0198.

Preparation of S3: Prepared from 4-chloro-2,6-dimethylaniline (1.55 g, 3.44 mmol) and bromoacetyl chloride (286 μL , 10.0 mmol) following the procedure detailed for **S1** providing **S3** (0.75 g, 28%) as a white powder: ^1H NMR (CDCl_3 , 300 MHz) δ

7.10 (s, 2H), 4.07 (s, 2H), 2.22 (s, 6H); ^{13}C NMR ($(\text{CD}_3)_2\text{SO}$, 125 MHz) δ 164.9, 137.5, 133.3, 130.7, 127.3, 29.1, 17.6; HRMS (FAB+) m/z : Calculated—277.9761, Found—277.9755.

Preparation of S4: A solution of **S1** (950 mg, 3.36 mmol) and 1-adamantylamine (760 mg, 5.0 mmol) in CH_3CN (10 mL) was treated with K_2CO_3 (700 mg, 5.1 mmol) and allowed to stir at 85 °C for 16 h. The reaction mixture was then filtered over celite and concentrated under reduced pressure. Flash chromatography (SiO_2 , 4% MeOH-DCM) provided S4 (1.11 g, 93%) as a white solid: ^1H NMR (CDCl_3 , 500 MHz) δ 9.04 (s, 1H), 6.93 (s, 2H), 3.42 (s, 2H), 2.54 (q, 4H, $J = 7.5$ Hz), 2.31 (s, 3H), 2.11 (br s, 3H), 1.58–1.73 (m, 13H), 1.17 (t, 6H, $J = 7.5$ Hz); ^{13}C NMR (CDCl_3 , 125 MHz) δ 172.2, 140.9, 137.1, 130.2, 127.2, 51.1, 44.1, 42.9, 36.5, 29.5, 25.1, 21.2, 14.7; HRMS (FAB+) m/z : Calculated—([M + H]) 355.2749, Found—355.2758 ([M + H]).

Preparation of S5: Prepared from **S2** (700 mg, 2.58 mmol) and 1-adamantylamine (590 mg, 3.9 mmol) following the procedure detailed for S4 providing S5 (800 mg, 91%) as an off-white solid: ^1H NMR (CDCl_3 , 500 MHz) δ 8.94 (s, 1H), 6.62 (s, 2H), 3.75 (s, 3H), 3.40 (s, 2H), 2.18 (s, 6H), 2.10 (br m, 3H), 1.57–1.71 (m, 13H); ^{13}C NMR (CDCl_3 , 125 MHz) δ 171.9, 158.1, 136.4, 127.0, 113.4, 55.3, 51.1, 44.0, 42.9, 36.5, 29.5, 18.9; HRMS (EI+) m/z : Calculated—342.2307, Found—342.2292.

Preparation of S6: Prepared from **S3** (750 mg, 2.73 mmol) and 1-adamantylamine (620 mg, 4.1 mmol) following the procedure detailed for S4 providing S6 (715 mg, 77%) as a white solid: ^1H NMR (CDCl_3 , 500 MHz) δ 9.06 (s, 1H), 7.05 (s, 2H), 3.41 (s, 2H), 2.18 (s, 6H), 2.10 (br m, 3H), 1.57–1.71 (m, 13H); ^{13}C NMR (CDCl_3 , 125

MHz) δ 171.6, 136.9, 132.8, 132.1, 128.0, 51.2, 44.1, 42.9, 36.5, 29.5, 18.6; HRMS (EI+) m/z : Calculated—347.1890, Found—347.1905.

Preparation of S7: Under an atmosphere of argon, a solution of **S4** (1.0 g, 2.82 mmol) in THF (15 mL) at 0 °C was treated with LiAlH₄ (325 mg, 8.5 mmol). The reaction mixture was allowed to warm to 25 °C and stirred at 65 °C for 36 h. The reaction mixture was allowed to cool to 0 °C and 1 mL H₂O and 1 mL NaOH were added slowly. The mixture was diluted with EtOAc, filtered, and partitioned between EtOAc-H₂O. The organic layer was dried (Na₂SO₄) and concentrated under reduced pressure providing **S7** (0.95 g, 99%) as a yellow oil: ¹H NMR (CDCl₃, 500 MHz) δ 6.88 (s, 2H), 2.98 (m, 2H), 2.85 (m, 2H), 2.70 (q, 4H, J = 7.5 Hz), 2.30 (s, 3H), 2.11 (br s, 3H), 1.62–1.74 (m, 13H), 1.27 (t, 6H, J = 7.5 Hz); ¹³C NMR (CDCl₃, 125 MHz) δ 142.88, 136.3, 131.5, 127.3, 51.1, 50.2, 43.0, 40.6, 36.8, 29.6, 24.4, 20.8, 15.0; HRMS (FAB+) m/z : Calculated—([M + H]) 341.2957, Found—341.2966 ([M + H]).

Preparation of S8: Prepared from **S5** (735 mg, 2.15 mmol) and LiAlH₄ (245 mg, 6.45 mmol) following the procedure detailed for **S7** providing **S8** (685 mg, 98%) as a yellow oil: ¹H NMR (CDCl₃, 500 MHz) δ 6.56 (s, 2H), 3.73 (s, 3H), 2.93 (dd, 2H, J = 6.5, 5.0 Hz), 2.79 (dd, 2H, J = 6.5, 5.0 Hz), 2.29 (s, 6H), 2.07 (br s, 3H), 1.58–1.71 (m, 13H); ¹³C NMR (CDCl₃, 125 MHz) δ 154.5, 139.8, 131.4, 113.8, 55.3, 50.2, 50.0, 43.0, 40.7, 36.8, 29.6, 18.8; HRMS (FAB+) m/z : Calculated—([M + H]) 329.2593, Found—329.2577 ([M + H]).

Preparation of S9: Prepared from **S6** (660 mg, 1.91 mmol) and LiAlH₄ (218 mg, 5.73 mmol) following the procedure detailed for **S7** providing **S9** (634 mg, 99%) as a yellow oil: ¹H NMR (CDCl₃, 500 MHz) δ 6.92 (s, 2H), 2.96 (m, 2H), 2.75 (m, 2H),

2.25 (s, 6H), 2.05 (br s, 3H), 1.58–1.71 (m, 13H); ^{13}C NMR (CDCl_3 , 125 MHz) δ 145.2, 130.4, 128.1, 125.5, 50.1, 49.2, 42.9, 40.3, 36.6, 29.5, 18.6; HRMS (FAB+) m/z : Calculated—($[\text{M} + \text{H}]$) 333.2098, Found—333.2094 ($[\text{M} + \text{H}]$).

Preparation of S10: A solution of **S7** (950 mg, 2.79 mmol) in Et_2O (5 mL) was treated with 2M HCl in Et_2O (2.80 mL) to provide a white solid that was filtered and dried. A solution of triethylorthoformate (5 mL) was added to this white solid and the mixture was allowed to stir at 120 °C for 30 min. The reaction mixture was concentrated under reduced pressure to provide an off-white powder that was filtered, washed with hexanes and dried to provide S10 (0.55 g, 52%) as a white powder: ^1H NMR (CDCl_3 , 500 MHz) δ 8.65 (s, 1H), 6.97 (s, 2H), 4.48 (t, 2H, J = 10.0 Hz), 4.31 (t, 2H, J = 10.0 Hz), 2.53–2.69 (m, 4H), 2.33 (s, 3H), 2.26 (br m, 3H), 2.10 (d, 6H, J = 2.5 Hz), 1.73 (t, 6H, J = 2.5 Hz), 1.26 (t, 6H, J = 7.5 Hz); ^{13}C NMR (CDCl_3 , 125 MHz) δ 156.2, 140.9, 140.3, 129.6, 127.6, 57.9, 52.1, 45.4, 41.0, 35.3, 29.1, 24.0, 21.3, 14.8; HRMS (FAB+) m/z : Calculated—($[\text{M}+]$) 351.2800, Found—351.2817 ($[\text{M}+]$).

Preparation of S11: Prepared from **S8** (685 mg, 2.10 mmol) and triethylorthoformate (5 mL) following the procedure detailed for S10 providing S11 (565 mg, 72%) as a white powder: ^1H NMR (CDCl_3 , 500 MHz) δ 9.04 (s, 1H), 6.49 (s, 2H), 4.27 (dd, 2H, J = 9.2, 12.3 Hz), 4.12 (dd, 2H, J = 9.2, 12.3 Hz), 3.66 (s, 3H), 2.21 (s, 6H), 2.13 (br m, 3H), 2.01 (d, 6H, J = 3.0 Hz), 1.62 (t, 6H, J = 2.8 Hz); ^{13}C NMR (CDCl_3 , 125 MHz) δ 159.7, 156.8, 137.0, 126.5, 114.0, 57.8, 55.3, 50.9, 45.1, 40.8, 35.3, 29.1, 18.4; HRMS (FAB+) m/z : Calculated—($[\text{M}+]$) 339.2436, Found—339.2448 ($[\text{M}+]$).

Preparation of S12: Prepared from S9 (630 mg, 1.91 mmol) and triethylorthoformate

(5 mL) following the procedure detailed for S10 providing S12 (600 mg, 83%) as a white powder: ^1H NMR (CDCl_3 , 500 MHz) δ 9.47 (s, 1H), 6.98 (s, 2H), 4.26 (m, 2H), 4.14 (m, 2H), 2.24 (s, 6H), 2.14 (br s, 3H), 2.01 (d, 6H, $J = 3.0$ Hz), 1.63 (t, 6H, $J = 3.2$ Hz); ^{13}C NMR (CDCl_3 , 125 MHz) δ 157.3, 137.7, 135.1, 132.3, 128.8, 58.1, 50.6, 45.1, 40.9, 35.3, 29.1, 18.2; HRMS (FAB+) m/z : Calculated—([M+]) 343.1941, Found—343.1932 ([M+]).

Preparation of S13: In a glove box, a solution of S10 (200 mg, 0.52 mmol) in hexanes (6 mL) was treated with KCOMe_2Et (75 mg, 0.57 mmol), and the mixture was allowed to stir at 35 °C for 1 h. The reaction mixture was then treated with $\text{RuCl}_2(\text{PCy}_3)(=\text{CH}-o\text{-O}^i\text{PrC}_6\text{H}_4)$ (312 mg, 0.52 mmol), removed from the glove box, and allowed to stir at 65 °C for 3 h. The precipitated solids were filtered and washed well with hexanes to provide S13 (335 mg, 96%) as a green powder: ^1H NMR (CDCl_3 , 500 MHz) δ 16.87 (s, 1H), 7.55 (ddd, 1H, $J = 1.7, 7.4, 8.8$ Hz), 7.15 (s, 2H), 6.91 (m, 2H), 6.83 (dd, 1H, $J = 1.5, 7.5$ Hz), 5.06 (hept, 1H, $J = 6.1$ Hz), 4.02 (dd, 2H, $J = 8.4, 11.4$ Hz), 3.85 (dd, 2H, $J = 8.4, 11.4$ Hz), 2.95 (br s, 6H), 2.70 (dq, 2H, $J = 7.6, 15.3$ Hz), 2.55 (dq, 2H, $J = 7.6, 15.3$ Hz), 2.53 (s, 3H), 2.41 (br s, 3H), 1.94 (d, 3H, $J = 12.0$ Hz), 1.83 (d, 3H, $J = 12.0$ Hz), 1.63 (d, 6H, $J = 6.1$ Hz), 1.13 (t, 6H, $J = 7.5$ Hz); ^{13}C NMR (CDCl_3 , 125 MHz) δ 311.7, 208.6, 152.4, 145.6, 143.1, 138.63, 138.59, 130.7, 127.1, 123.6, 122.6, 113.3, 74.2, 57.7, 52.8, 44.5, 42.2, 36.2, 30.0, 23.3, 22.5, 21.7, 14.1; HRMS (FAB+) m/z : Calculated—670.2031, Found—670.2019.

Preparation of S14: Prepared from S11 (100 mg, 0.27 mmol) and $\text{RuCl}_2(\text{PCy}_3)(=\text{CH}-o\text{-O}^i\text{PrC}_6\text{H}_4)$ (160 mg, 0.27 mmol) following the procedure detailed for S13 providing S14 (138 mg, 78%) as a green powder: ^1H NMR (CDCl_3 , 500 MHz) δ

16.98 (s, 1H), 7.56 (ddd, 1H, $J = 1.9, 7.2, 8.9$ Hz), 6.93 (m, 3H), 6.78 (s, 2H), 5.09 (hept, 1H, $J = 6.1$ Hz), 4.04 (dd, 2H, $J = 8.5, 11.9$ Hz), 1.89 (s, 3H), 3.85 (dd, 2H, $J = 8.5, 11.9$ Hz), 2.95 (br s, 6H), 2.41 (s, 3H), 2.26 (s, 6H), 1.93 (d, 3H, $J = 12.0$ Hz), 1.83 (d, 3H, $J = 12.0$ Hz), 1.63 (d, 6H, $J = 6.0$ Hz); ^{13}C NMR (CDCl_3 , 125 MHz) δ 312.4, 208.3, 159.4, 152.4, 145.92, 145.90, 139.6, 135.3, 130.8, 124.0, 122.8, 114.0, 113.3, 74.2, 57.2, 55.7, 51.3, 44.6, 42.2, 36.2, 30.0, 22.5, 18.8; HRMS (FAB+) m/z : Calculated—658.1667, Found—658.1645.

Preparation of S15: Prepared from **S12** (100 mg, 0.27 mmol) and $\text{RuCl}_2(\text{PCy}_3)(=\text{CH}-o\text{-O}^i\text{PrC}_6\text{H}_4)$ (160 mg, 0.27 mmol) following the procedure detailed for S13 providing S15 (136 mg, 78%) as a green powder: ^1H NMR (CDCl_3 , 500 MHz) δ 16.89 (s, 1H), 7.59 (m, 1H), 7.26 (m, 2H), 6.96 (m, 3H), 5.10 (hept, 1H, $J = 6.2$ Hz), 4.05 (dd, 2H, $J = 8.4, 11.6$ Hz),), 3.83 (dd, 2H, $J = 8.5, 11.6$ Hz), 2.93 (br s, 6H), 2.41 (s, 3H), 2.28 (s, 6H), 1.93 (d, 3H, $J = 12.0$ Hz), 1.84 (d, 3H, $J = 12.5$ Hz), 1.63 (d, 6H, $J = 6.0$ Hz); ^{13}C NMR (CDCl_3 , 125 MHz) δ 310.8, 208.2, 152.4, 145.8, 140.7, 140.4, 133.9, 131.0, 128.8, 124.0, 122.9, 113.3, 74.3, 57.4, 50.9, 44.7, 42.1, 36.1, 30.0, 22.4, 18.4; HRMS (FAB+) m/z : Calculated—664.1143, Found—664.1151.

Preparation of 6.25: In a glovebox, a solution of **S13** (98 mg, 0.14 mmol) and THF (5 mL) was treated with AgOPiv (92 mg, 0.44 mmol). The reaction mixture was allowed to stir at 25 °C for 30 min and a color change from brown to purple was observed. The mixture was immediately filtered over celite and concentrated. The residue was triturated with Et_2O and dried to provide a purple solid. The purple solid was then taken up in THF (3 mL), treated with NH_4NO_3 (350 mg, 4.4 mmol)

and allowed to stir for 1 h. The reaction mixture was concentrated, taken up in benzene, and filtered over celite. The filtrate was dried and triturated with Et₂O until the washes were colorless providing **6.25** (30 mg, 31%) as a purple powder: ¹H NMR (C₆D₆, 500 MHz) δ 15.19 (s, 1H), 7.42 (dd, 1H, *J* = 1.5, 7.5 Hz) 7.18 (ddd, 1H, *J* = 1.5, 7.5, 8.5 Hz), 7.06 (d, 1H, *J* = 1.0 Hz), 6.83 (dt, 1H, *J* = 1.0, 7.5 Hz), 6.79 (d, 1H, *J* = 1.5 Hz), 6.47 (d, 1H, *J* = 8.5 Hz), 4.55 (hept, 1H, *J* = 6.3 Hz), 4.18 (s, 1H), 3.55 (q, 1H, *J* = 10.7 Hz), 3.39 (m, 1H), 3.17–3.29 (m, 2H), 3.06 (dq, 1H, *J* = 7.7, 15.3 Hz), 2.86–3.00 (m, 2H), 2.63 (dq, 1H, *J* = 7.5, 15.0 Hz), 2.24 (m, 1H), 2.15 (s, 3H), 2.10 (m, 1H), 1.96–2.02 (m, 2H), 1.89 (d, 1H, *J* = 11.0 Hz), 1.77 (dd, 1H, *J* = 1.5, 12.0 Hz), 1.66 (m, 1H), 1.44–1.55 (m, 3H), 1.42 (d, 3H, *J* = 6.5 Hz), 1.28 (t, 3H, *J* = 7.5 Hz), 1.20 (t, 3H, *J* = 7.5 Hz), 1.10 (m, 2H), 0.94 (d, 3H, *J* = 6.0 Hz), 0.59 (d, 1H, *J* = 12.0 Hz); ¹³C NMR (C₆D₆, 100 MHz) δ 214.3, 154.7, 143.54, 143.50, 141.1, 137.8, 134.9, 128.5, 127.0, 126.8, 123.37, 123.33, 113.0, 74.3, 66.7, 63.0, 52.9, 43.0, 41.8, 40.3, 37.9, 37.77, 37.73, 33.3, 30.9, 29.8, 24.1, 23.4, 21.4, 21.2, 20.2, 15.7, 15.3; HRMS (FAB+) *m/z*: Calculated—661.2454, Found—661.2422.

Preparation of 9: Prepared from **S14** (118 mg, 0.179 mmol) and AgOPiv (112 mg, 0.54 mmol) following the procedure detailed for **6.25** providing **6.26** (16.5 mg, 14%) as a purple powder: ¹H NMR (C₆D₆, 400 MHz) δ 15.21 (s, 1H), 7.37 (dd, 1H, *J* = 1.6, 7.6 Hz), 7.19 (m, 1H), 6.82 (m, 2H), 6.44 (d, 1H, *J* = 2.8 Hz), 6.49 (d, 1H, *J* = 8.4 Hz), 4.58 (hept, 1H, *J* = 6.3 Hz), 4.16 (s, 1H), 3.40 (m, 1H), 3.33 (s, 3H), 3.10–3.30 (m, 3H), 2.37 (d, 6H, *J* = 2.8 Hz), 2.24 (m, 1H), 2.11 (m, 1H), 1.96–2.01 (m, 2H), 1.85–1.92 (m, 1H), 1.73–1.81 (m, 1H), 1.65 (m, 1H), 1.48 (m, 3H), 1.44 (d, 3H, *J* = 6.4 Hz), 1.06 (m, 2H), 0.97 (d, 3H, *J* = 6.0 Hz), 0.58 (d, 1H, *J* = 12.4

Hz); ^{13}C NMR (C_6D_6 , 100 MHz) δ 214.4, 159.2, 154.7, 143.6, 139.3, 137.0, 131.8, 128.5, 126.8, 123.38, 123.35, 114.2, 113.0, 74.3, 66.7, 63.0, 54.8, 51.5, 43.1, 41.8, 40.3, 37.9, 37.8, 37.6, 33.3, 30.9, 29.8, 21.2, 20.2, 18.8, 17.8; HRMS (FAB+) m/z : Calculated—648.2012, Found—648.2036.

Preparation of 6.25: Prepared from **S15** (195 mg, 0.294 mmol) and AgOPiv (185 mg, 0.865 mmol) following the procedure detailed for **6.25** providing **6.27** (55 mg, 28%) as a purple powder: ^1H NMR (C_6D_6 , 400 MHz) δ 15.08 (s, 1H), 7.36 (dd, 1H, J = 1.6, 7.6 Hz), 7.16–7.24 (m, 2H), 6.81–6.87 (m, 2H), 6.51 (d, 1H, J = 8.4 Hz), 4.58 (hept, 1H, J = 6.2 Hz), 4.09 (s, 1H), 3.10–3.33 (m, 4H), 2.21 (m, 1H), 2.19 (d, 6H, J = 6.0 Hz), 2.10 (m, 1H), 1.96 (m, 1H), 1.85 (m, 2H), 1.75 (m, 1H), 1.63 (m, 1H), 1.46 (m, 3H), 1.41 (d, 3H, J = 6.4 Hz), 1.07 (m, 2H), 0.96 (d, 3H, J = 6.0 Hz), 0.54 (d, 1H, J = 12.4 Hz); ^{13}C NMR (C_6D_6 , 100 MHz) δ 265.9, 214.2, 154.7, 143.5, 140.0, 138.0, 137.4, 133.4, 129.2, 128.6, 127.1, 123.4, 123.3, 113.0, 74.4, 66.7, 63.2, 51.0, 43.0, 41.8, 40.2, 37.8, 37.7, 37.6, 33.2, 30.9, 29.7, 21.2, 20.2, 18.3, 17.3; HRMS (FAB+) m/z : Calculated—652.1517, Found—652.1529.

General Procedure for Homodimerization Reactions: In a glovebox, a 1 mL volumetric flask was charged with catalyst (0.0981 mmol) and filled to the line with THF to create a stock solution (0.0981 M). A portion of the catalyst stock solution (50 μL , ca. 5 μmol) was added to a 4 mL vial containing substrate (5 mmol) and THF (1.1 mL, ca. 3 M). The vial was placed into an aluminum block (IKA #3904400) preheated to 35 $^\circ\text{C}$ using a temperature controlled hotplate and the reaction was stirred while open to the glovebox atmosphere. After completion of the reaction (determined by ^1H NMR spectroscopy), the vial was removed from the glovebox,

quenched with oxygen, and the product was isolated via flash chromatography on silica gel according to literature procedures.⁴⁷ The percentage of Z-olefin product was determined by ¹H and ¹³C NMR spectroscopy, and all spectra were consistent with previous literature reports.³

General Procedure for Determination of Initiation Rates: In a glovebox, a 1 mL volumetric flask was charged with **6.2** (8.1 mg, 0.012 mmol) and filled to the line with C₆D₆ to create a stock solution (ca. 0.012 M). A portion of the stock solution (0.25 mL, 0.003 mmol **6.2**) was added to a NMR tube and diluted with C₆D₆ (0.35 mL). The NMR tube was sealed with a septa cap and placed in the NMR spectrometer at 30 °C. Butyl vinyl ether (12 μL, 0.09 mmol) was added and the disappearance of the benzyldiene proton resonance was monitored by arraying the 'pad' function in VNMRj.

All reactions, with the exception of **6.23**, showed clean first-order kinetics over a period of at least three half-lives. Spectra were baseline corrected and integrated with MestReNova. Estimation of error was determined from the average of three different kinetic runs.

General Procedure for Cross-Metathesis of 6.3 and 6.4: In a glovebox, a 4 mL vial was charged with **6.3** (1.33 mL, 10 mmol) and tridecane (internal standard, 1.22 mL, 5 mmol). A portion (89 μL, 0.35 mmol **6.3**) of this stock solution was added to a second 4 mL vial followed by **6.4** (111 μL, 0.69 mmol) and THF (0.45 mL). This mixture was stirred for several minutes before taking a t₀ timepoint. An aliquot (50 μL, 0.0035 mmol) of a catalyst solution prepared from **6.24** (44 mg, 0.069 mmol)

in THF (1 mL) was added to the substrate solution and the vial was sealed and heated to the desired temperature. Periodically, the reaction was cooled to RT, and an aliquot (20 μ L) was removed from the glovebox, diluted with a solution of ethyl vinyl ether in CH_2Cl_2 , and analyzed via GC.

GC response factors for all starting materials and products (ethylene excluded) were obtained in order to determine accurate conversions and the GC data was worked up according to the literature.²¹

GC instrument conditions: Inlet temperature—250 °C; Detector temperature—250 °C; hydrogen flow—32 mL/min; air flow—400 mL/min; constant col + makeup flow—30 mL/min.

GC Method: 50 °C for 5 min, followed by a temperature increase of 10 °C/min to 240 °C and a subsequent isothermal period at 240 °C for 5 min (total run time = 29 min).

Preparation of 6.28: To benzoic acid (0.305 g, 2.50 mmol) and NaOH (0.104 g, 2.60 mmol) was added H_2O (3 mL) and the solution was stirred at RT for 15 min. A solution of AgNO_3 (0.35 g, 2.08 mmol) in H_2O (3 mL) was added drop-wise which resulted in immediate precipitation of a white solid. The suspension was stirred for 15 min, after which the white precipitate was collected on a medium porosity frit and washed with H_2O , MeOH, and Et_2O . **6.28-Ag** was recovered as a light gray solid (0.51 g, 90%). ^1H NMR (400 MHz, $\text{dms}\text{-d}_6$) δ 8.06–7.83 (m, 2H), 7.54–7.14 (m, 3H).

Catalyst **6.28** (26 mg, 87%) was prepared in a manner analogous to **6.19**.

6.18 (30 mg, 0.043 mmol), **6.28-Ag** (15 mg, 0.065 mmol) and THF (3 mL). ^1H NMR (300 MHz, C_6D_6) δ 15.07 (s, 1H), 8.10 (s, 2H), 7.98–7.91 (m, 1H), 7.50 (s, 1H) 7.44–7.41 (m, 1H), 6.93–6.73 (m, 3H), 6.59 (d, J = 8.6 Hz, 1H), 6.25 – 6.20 (m, 1H), 6.16 (s, 1H), 4.73–4.65 (m, 1H), 4.25 (s, 1H), 3.44 (s, 1H), 3.29 (s, 2H), 2.51 (s, 2H), 2.46 (s, 1H), 2.29 (s, 1H), 2.11 (d, J = 8.5 Hz, 4H), 1.73 (s, 2H), 1.57 (d, J = 6.3 Hz, 3H), 1.42 (s, 1H), 1.38–1.31 (m, 4H), 0.92 (d, J = 6.3 Hz, 3H), 0.83 (d, J = 6.1 Hz, 1H).

Preparation of 6.29: **6.29-Ag** (0.34 g, 56%) was prepared in an analogous manner to **6.28-Ag**. P-toluic acid (0.340 g, 2.50 mmol), NaOH (104 mg, 2.6 mmol), AgNO_3 (350 mg, 2.08 mmol). ^1H NMR (400 MHz, $\text{dms}\text{-}d_6$) δ 7.84 (d, J = 7.8 Hz, 2H), 7.17 (d, J = 7.8 Hz, 2H), 2.33 (s, 3H).

Catalyst **6.29** (15.7 mg, 52%) was prepared in a manner analogous to **6.19**. **6.18** (30 mg, 0.043 mmol), **6.29-Ag** (16 mg, 0.065 mmol), and THF (3 mL). ^1H NMR (300 MHz, C_6D_6) δ 15.06 (s, 1H), 8.07 (d, J = 7.9 Hz, 2H), 7.50 (d, J = 5.8 Hz, 1H), 7.27–7.20 (m, 1H), 6.98 (d, J = 7.9 Hz, 2H), 6.89 (t, J = 7.2 Hz, 1H), 6.79 (s, 1H), 6.60 (d, J = 8.2 Hz, 1H), 6.23 (s, 1H), 4.78–4.63 (m, 1H), 4.29 (s, 1H), 3.45 (t, J = 9.9 Hz, 1H), 3.31 (ddd, J = 20.3, 13.2, 7.8 Hz, 3H), 2.50 (d, J = 9.2 Hz, 3H), 2.16–2.04 (m, 9H), 1.59 (d, J = 6.3 Hz, 4H), 1.41–1.15 (m, 3H), 0.94 (d, J = 6.1 Hz, 2H), 0.88 (d, J = 6.1 Hz, 1H).

Preparation of 6.30: **6.30-Ag** (0.34 g, 56%) was prepared in an analogous manner to **6.28-Ag**. 4-fluorobenzoic acid (325 mg, 2.25 mmol), NaOH (94 mg, 2.34 mmol), AgNO_3 (318 mg, 1.88 mmol).

Catalyst **6.30** (13.5 mg, 44%) was prepared in a manner analogous to **6.19**.

6.18 (30 mg, 0.043 mmol), **6.30-Ag** (15 mg, 0.065 mmol), THF (3 mL). ^1H NMR (300 MHz, C_6D_6) δ 15.06 (s, 1H), 7.95 (s, 1H), 7.81–7.72 (m, 1H), 7.48 (d, J = 5.7 Hz, 1H), 7.44–7.40 (m, 1H), 7.24 (s, 1H), 6.91–6.56 (m, 4H), 6.19–6.13 (m, 1H), 6.09 (s, 1H), 4.72–4.65 (m, 1H), 4.22 (s, 1H), 3.42 (s, 1H), 2.49 (s, 1H), 2.43 (s, 1H), 2.24 (s, 1H), 2.05 (d, J = 13.7 Hz, 3H), 1.72 (s, 1H), 1.57 (d, J = 6.4 Hz, 2H), 1.42 (s, 1H), 1.40–1.29 (m, 3H), 0.92 (d, J = 6.2 Hz, 2H), 0.84 (d, J = 6.1 Hz, 1H).

Preparation of 6.31: **6.31-Ag** (1.14 g, 96%) was prepared in an analogous manner to **6.28-Ag**. 4-hydroxybenzoic acid (354 mg, 2.50 mmol), NaOH (104 mg, 2.60 mmol), AgNO_3 (352 mg, 2.08 mmol).

Catalyst **6.31** (12 mg, 58%) was prepared in a manner analogous to **6.19**. **6.18** (20 mg, 0.029 mmol), **6.31-Ag** (10.5 mg, 0.043 mmol), and THF (3 mL). ^1H NMR (300 MHz, C_6D_6) δ 15.20–14.86 (m, 1H), 8.00–7.92 (m, 2H), 7.52–7.38 (m, 2H), 6.93–6.86 (m, 2H), 6.80–6.73 (m, 1H), 6.58–6.45 (m, 2H), 6.26–6.21 (m, 1H), 4.26 (s, 2H), 2.51 (s, 3H), 2.13 (d, J = 6.5 Hz, 8H), 1.59 (d, J = 6.4 Hz, 5H), 1.12 (s, 1H), 0.95 (d, J = 6.0 Hz, 3H), 0.30 (s, 1H).

Preparation of 6.36: A 100 mL RB was charged with picolinic acid (0.56 g, 4.57 mmol) and silver (I) oxide (0.64 g, 2.74 mmol). MeCN (20 mL) and H_2O (6 mL) were added and the solution was stirred for 3 h under argon while shielded from light. After this time, the solution was filtered and the filtrate washed with copious amounts of MeCN. The supernatant was concentrated, washed with hexanes, and the collected by filtration as a white powder (**6.36-Ag**, 140 mg, 13% yield) that was used without further purification.

In a glovebox, a 20 mL vial was charged with **6.18** (26 mg, 0.037 mmol)

and **6.36-Ag** (9 mg, 0.041 mmol). THF was added and the solution was stirred for 1 h at RT. Workup was analogous to **6.19** to give **6.36** (20 mg, 78% yield) as a thermally unstable green powder. ^1H NMR (400 MHz, C_6D_6) δ 15.28 (s, 1H), 8.13 (d, $J = 7.6$ Hz, 1H), 7.53 (d, $J = 9.2$ Hz, 1H), 7.20 (m, 1H), 6.90 (d, $J = 8$ Hz, 1H), 6.84 (t, $J = 7.6$ Hz, 1H), 6.74 (t, $J = 9.2$ Hz, 1H), 6.44 (d, $J = 8.4$ Hz, 1H), 6.26 (s, 1H), 5.94 (s, 1H), 5.65 (m, 1H), 5.07 (s, 1H), 4.56 (sept, $J = 6.4$ Hz, 1H), 3.33 (m, 3H), 3.19 (m, 1H), 2.35 (s, 4H), 2.28 (br s, 3H), 2.18 (m, 1H), 2.06 (s, 3H), 1.97 (m, 1H), 1.83 (br s, 1H), 1.72 (s, 3H), 1.65 (br s, 3H), 1.39 (m, 1H), 1.24 (m, 4H), 0.83 (m, 1H), 0.39 (d, $J = 6.4$ Hz, 3H). Upon dissolving in C_6D_6 and heating to 70 °C, **6.36** would cleanly decompose into a mixture of yellow-colored hydride species identified by equal intensity resonances at δ –6.64 and –9.98 ppm. These species did not exchange on the NMR timescale, and were indefinitely stable under an inert atmosphere. **6.36** also decomposed in the solid state over a period of several days.

Preparation of 6.37: In a glovebox, a Schlenk flask was charged with **6.2** (24 mg, 0.036 mmol) and *p*-benzoquinone (16 mg, 0.15 mmol). THF (2 mL) was added which resulted in an immediate color change from purple to red/orange. The flask was sealed, removed from the glovebox, and heated to 70 °C for 12 h. After cooling to RT, the reaction was concentrated and the flask was taken back into the glovebox, where the red/brown residue was triturated with Et_2O to give **6.37** (6 mg, 13%) as a red crystalline solid. ^1H NMR (500 MHz, CD_2Cl_2) δ 7.16 (t, $J = 8.0$ Hz, 2H), 7.08 (t, $J = 7.5$ Hz, 2H), 6.92 (br s, 4H), 6.82 (t, $J = 9.0$ Hz, 4H), 6.77 (br s, 2H), 6.65 (s, 4H), 5.14 (s, 2H), 4.77 (dd, $J = 7.5, 2.5$ Hz, 2H), 4.58 (sept, $J = 6.0$ Hz, 2H), 4.19

(dd, $J = 7.5, 2.5$ Hz, 2H), 3.67 (quin, $J = 9.5$ Hz, 2H), 3.61–3.57 (m, 4H), 3.42 (t, $J = 10.0$ Hz, 2H), 3.19 (dd, $J = 7.5, 3.0$ Hz, 2H), 3.01 (br s, 2H), 2.83 (br d, $J = 12.5$ Hz, 2H), 2.43 (s, 6H), 2.16 (br d, $J = 9.0$ Hz, 2H), 2.1–2.08 (m, 2H), 2.06 (s, 6H), 1.93 (br s, 2H), 1.89 (s, 6H), 1.76 (br d, $J = 11.5$ Hz, 2H), 1.69–1.66 (m, 2H), 1.62–1.59 (m, 2H), 1.49 (br d, $J = 11.5$ Hz, 2H), 1.40–1.38 (m, 2H), 1.35–1.32 (m, 2H), 1.22 (d, $J = 6.0$ Hz, 6H), 1.19 (d, $J = 5.5$ Hz, 6H). ^{13}C NMR (126 MHz, CD_2Cl_2) δ 211.45, 163.30, 156.08, 150.53, 138.87, 137.96, 136.29, 135.59, 134.37, 129.98, 129.62, 129.45, 125.98, 119.24, 116.50, 113.50, 90.42, 88.63, 80.35, 77.04, 69.27, 65.11, 58.66, 46.11, 42.07, 41.30, 40.00, 38.66, 37.44, 31.97, 30.63, 29.30, 22.36, 22.27, 21.98, 19.42, 17.64. HRMS (FAB⁺): A mass corresponding to the monomeric species was detected. Calculated—679.2474, Found—679.2458.

General Polymerization Procedure: In a glovebox, a stock solution of catalyst was prepared from **6.24** (78 mg, 0.123 mmol) and THF (1 mL). An aliquot (50 μL , 0.0062 mmol **6.24**) of stock solution was added to a Schlenk flask and diluted with THF (0.5 mL). On a vacuum manifold, a separate Schlenk flask was flame-dried and charged with monomer (0.62 mmol) and THF (2 mL). The monomer solution was degassed via freeze-pump-thaw (3X) and the catalyst solution was injected via gas-tight syringe under argon at a given temperature. After stirring for 1 h, the polymerization was quenched with ethyl vinyl ether (0.1 mL) and, unless otherwise specified, precipitated into vigorously stirred MeOH. The precipitate was collected by vacuum filtration using either a medium or fine porosity frit and dried under vacuum.

References

- (1) (a) Fürstner, A. *Angew. Chem. Int. Ed.* **2000**, 39, 3012. (b) Trnka, T. M.; Grubbs, R. H. *Acc. Chem. Res.* **2001**, 34, 18. (c) Astruc, D. *New J. Chem.* **2005**, 29, 42.
- (2) Grubbs, R.H. *Handbook of Metathesis*, Wiley-VCH, Weinheim, **2003**.
- (3) (a) Jiang, A. J.; Zhao, Y.; Schrock, R. R.; Hoveyda, A. H. *J. Am. Chem. Soc.* **2009**, 131, 16630. (b) Marinescu, S. C.; Schrock, R. R.; Müller, P.; Takase, M. K.; Hoveyda, A. H. *Organometallics* **2011**, 30, 1780. (c) Meek, S. J.; O'Brien, R. V.; Llaveria, J.; Schrock, R. R.; Hoveyda, A. H. *Nature* **2011**, 471, 461. (d) Marinescu, S. C.; Levine, D. S.; Zhao, Y.; Schrock, R. R.; Hoveyda, A. H. *J. Am. Chem. Soc.* **2011**, 133, 11512.
- (4) (a) Wang, Y.; Jimenez, M.; Hansen, A. S.; Raiber, E.-A.; Schreiber, S. L.; Young, D. W. *J. Am. Chem. Soc.* **2011**, 133, 9196. (b) Gallenkamp, D.; Fürstner, A. *J. Am. Chem. Soc.* **2011**, 133, 9232.
- (5) (a) McNeill, K.; Anderson, R. A.; Bergman, R. G. *J. Am. Chem. Soc.* **1995**, 117, 3625. (b) McNeill, K.; Anderson, R. A.; Bergman, R. G. *J. Am. Chem. Soc.* **1997**, 119, 11244. (c) Trnka, T. M.; Day, M. W.; Grubbs, R. H. *Organometallics* **2001**, 20, 3845.
- (6) Endo, K.; Grubbs, R. H. *J. Am. Chem. Soc.* **2011**, 133, 8525.
- (7) (a) Hong, S. H.; Chlenov, A.; Day, M. W.; Grubbs, R. H. *Angew. Chem. Int. Ed.* **2007**, 46, 5148. (b) Hong, S. H.; Day, M. W.; Grubbs, R. H. *J. Am. Chem. Soc.* **2004**, 126, 7414. (c) Hong, S. H.; Wenzel, A. G.; Salguero, T. T.; Day, M. W.; Grubbs, R. H. *J. Am. Chem. Soc.* **2007**, 129, 7961. (d) Vehlouw, K.; Gessler, S.; Blechert, S.

Angew. Chem. Int. Ed. **2007**, *46*, 8082. (e) Leitao, E. M.; Dubberley, S. R.; Piers, W. E.; Wu, Q.; McDonald, R. *Chem. Eur. J.* **2008**, *14*, 11565. (f) Poater, A.; Cavallo, L.; *J. Mol. Catal. A: Chem.* **2010**, *324*, 75. (g) Poater, A.; Ragone, F.; Correa, A.; Cavallo, L. *J. Am. Chem. Soc.* **2009**, *131*, 9000. (h) Mathew, J.; Koga, N.; Suresh, C. H. *Organometallics* **2008**, *27*, 4666. (i) Rensburg, W. J.; Steynberg, P. J.; Meyer, W. H.; Kirk, M. M.; Forman, G. S. *J. Am. Chem. Soc.* **2004**, *126*, 14332.

(8) (a) Sanford, M. S.; Love, J. A.; Grubbs, R. H. *J. Am. Chem. Soc.* **2001**, *123*, 6543. (b) Hejl, A. PhD. Dissertation, California Institute of Technology, **2007**. (c) Vorfalt, T.; Wannowius, K.-J.; Plenio, H. *Angew. Chem. Int. Ed.* **2010**, *1*, 5533. (d) Ashworth, I. W.; Hillier, I. H.; Nelson, D. J.; Percy, J. M.; Vincent, M. A. *Chem. Comm.* **2011**, *47*, 5428. (e) Thiel, V.; Hendann, M.; Wannowius, K.-J.; Plenio, H. *J. Am. Chem. Soc.* **2012**, *134*, 1104.

(9) Schrock, R. R.; Jiang, A. J.; Marinescu, S. C.; Simpson, J. H.; Müller, P. *Organometallics* **2010**, *29*, 6816.

(10) A small amount (ca. 15%) of migration was also observed for **6.10** although in this case, it did not appear to inhibit the cross-metathesis reaction.

(11) Hong, S. H.; Sanders, D. P.; Lee, C. W.; Grubbs, R. H. *J. Am. Chem. Soc.* **2005**, *127*, 17160.

(12) (a) Schmidt, B. *Eur. J. Org. Chem.* **2003**, *34*, 816. (b) Alcaide, B.; Almendros, P.; Luna, A. *Chem. Rev.* **2009**, *109*, 3817. (c) Donohoe, T. J.; O'Riordan, T. J. C.; Rosa, C. P. *Angew. Chem. Int. Ed.* **2009**, *48*, 1014. (d) Gauthier, D.; Lindhardt, A. T.; Olsen, E. P. K.; Overgaard, J.; Skrydstrup, T. *J. Am. Chem. Soc.* **2010**, *132*, 7998.

- (13) A vent to an inert atmosphere was sufficient.
- (14) Catalyst **6.2** was only sparingly soluble in MeOH.
- (15) (a) Romero, P. E.; Piers, W. E.; McDonald, R. *Angew. Chem. Int. Ed.* **2004**, 43, 6161. (b) Wenzel, A. G.; Grubbs, R. H. *J. Am. Chem. Soc.* **2006**, 128, 16048. (c) Romero, P. E.; Piers, W. E. *J. Am. Chem. Soc.* **2007**, 129, 1698. (d) Rowley, C. N.; Eide, E. F. van der; Piers, W. E.; Woo, T. K. *Organometallics* **2008**, 27, 6043. (e) Eide, E. F. van der; Romero, P. E.; Piers, W. E. *J. Am. Chem. Soc.* **2008**, 130, 4485. (f) Leita, E. M.; Eide, E. F. van der; Romero, P. E.; Piers, W. E.; McDonald, R. *J. Am. Chem. Soc.* **2010**, 132, 2784. (g) Eide, E. F. van der; Piers, W. E. *Nature Chemistry*. **2010**, 2, 571. (h) Keitz, B. K.; Grubbs, R. H. *J. Am. Chem. Soc.* **2011**, 133, 16277.
- (16) Herbert, M. B.; Lan, Y.; Keitz, B. K.; Liu, P.; Endo, K.; Day, M. W.; Houk, K. N.; Grubbs, R. H. *J. Am. Chem. Soc.* **2012**, 134, 7861.
- (17) (a) Keitz, B. K.; Grubbs, R. H. *unpublished results*. (b) Theriot, J. C. Undergraduate Senior thesis, California Institute of Technology, 2012.
- (18) Nyman, M. D.; Hampden-Smith, M. J.; Duesler, E. N. *Inorg. Chem.* **1997**, 36, 2218.
- (19) Liu, P.; Xu, X.; Dong, X.; Keitz, B. K.; Herbert, M. B.; Grubbs, R. H.; Houk, K. N. *J. Am. Chem. Soc.* **2012**, 134, 1464.
- (20) Catalyst **6.21** was not examined.
- (21) Ritter, T.; Hejl, A.; Wenzel, A. G.; Funk, T. W.; Grubbs, R. H. *Organometallics* **2006**, 25, 5740.
- (22) Krause, J. O.; Nuyken, O.; Wurst, K.; Buchmeiser, M. R. *Chem. Eur. J.* **2004**,

10, 777.

(23) (a) Jović, M.; Torker, S.; Chen, P. *Organometallics* **2011**, *30*, 3971. (b) Buchmeiser, M. R.; Ahmad, I.; Gurram, V.; Kumar, P. S. *Macromolecules* **2011**, *44*, 4098.

(24) (a) Buchowicz, W.; Mol, J. C.; Lutz, M.; Spek, A. L. *J. Organomet. Chem.* **1999**, *588*, 205. (b) Buchowicz, W.; Ingold, F.; Mol, J. C.; Lutz, M.; Spek, A. L. *Chem. Eur. J.* **2001**, *7*, 2842. (c) Krause, J. O.; Nuyken, O.; Wurst, K.; Buchmeiser, M. R. *Chem. Eur. J.* **2004**, *10*, 777. (d) Kumar, P. S. Wurst, K.; Buchmeiser, M. R. *J. Am. Chem. Soc.* **2009**, *131*, 387.

(25) For a discussion of the effect of the NHC aryl group on ruthenium metathesis catalysts see: Süßner, M.; Plenio, H. *Chem. Comm.* **2005**, 5417.

(26) For selected examples of olefin migration/isomerization catalyzed by ruthenium hydrides see: (a) Bourgeois, D.; Pancrazi, A.; Nolan, S. P.; Prunet, J. *J. Organomet. Chem.* **2002**, *643/644*, 247. (b) Sworen, J. C.; Pawlow, J. H.; Case, W.; Lever, J.; Wagener, K. B. *J. Mol. Catal. A: Chem.* **2003**, *194*, 69. (c) Krompiec, S.; Kuźnik, N.; Penczek, R.; Rzepa, J.; Mrowiec-Białon, J. *J. Mol. Catal. A: Chem.* **2004**, *219*, 29. (d) Krompiec, S.; Kuźnik, N.; Krompiec, M.; Penczek, R.; Mrzigod, J.; Tórz, A. *J. Mol. Catal. A: Chem.* **2006**, *253*, 132. (e) Faller, J. W.; Fontaine, P. *Organometallics* **2007**, *26*, 1738. (f) Alcaide, B.; Almendros, P.; Luna, A. *Chem. Rev.* **2009**, *109*, 3817.

(27) Some additives, like 1,4-benzoquinone, led to immediate catalyst decomposition, while milder compounds, such as α,α -dichlorotoluene, resulted in decreased reaction conversions.

- (28) (a) Hamilton, J. G.; Ivin, K. J.; Rooney, J. J. *J. Mol. Catal.* **1985**, *28*, 255.
 (b) Cobo, N.; Esteruelas, M. A.; Gonzalez, F.; Herrero, J.; Lopez, A.M.; Lucio, P.; Olivan, M. *J. Catal.* **2004**, *223*, 319.
- (29) (a) Flook, M. M.; Jiang, A. J.; Schrock, R. R.; Hoveyda, A. H. *J. Am. Chem. Soc.* **2009**, *131*, 7962. (b) Flook, M. M.; Ng, V. W. L.; Schrock, R. R. *J. Am. Chem. Soc.* **2011**, *133*, 1784. (c) Schrock, R. R. *J. Chem. Soc., Dalton Trans.* **2011**, *40*, 7484.
- (30) (a) Delaude, L.; Demonceau, A.; Noels, A. F. *Macromolecules* **1999**, *32*, 2091.
 (b) Amir-Ebrahimi, V.; Corry, D. A.; Hamilton, J. G.; Thompson, J. M.; Rooney, J. *J. Macromolecules* **2000**, *33*, 717. (c) Delaude, L.; Demonceau, A.; Noels, A. F. *Macromolecules* **2003**, *36*, 1446. (d) Peeck, L. H.; Leuthäusser, S.; Plenio, H. *Organometallics* **2010**, *29*, 4339.
- (31) (a) Lin, W.-Y.; Murugesu, M. G.; Sudhakar, S.; Yang, H.-C.; Tai, H.-C.; Chang, C.-S.; Liu, Y.-H.; Wang, Y.; Chen, I.-W. P.; Chen, C.-H.; Luh, T.-Y. *Chem. Eur. J.* **2005**, *12*, 324. (b) Lee, J. C.; Parker, K. A.; Sampson, N. S. *J. Am. Chem. Soc.* **2006**, *128*, 4578. (c) Chou, C.-M.; Lee, S.-L.; Chen, C.-H.; Biju, A. T.; Wang, H.-W.; Wu, Y.-L.; Zhang, G.-F.; Yang, K.-W.; Lim, T.-S.; Huang, M.-J.; Tsai, P.-Y.; Lin, K.-C.; Huang, S.-L.; Chen, C.-H.; Luh, T.-Y. *J. Am. Chem. Soc.* **2009**, *131*, 12579. (d) Leitgeb, A.; Wappel, J.; Slugovc, C. *Polymer* **2010**, *51*, 2927.
- (32) (a) Weskamp, T.; Kohl, F.J.; Herrmann, W.A. *J. Organomet. Chem.* **1999**, *582*, 362. (b) Hamilton, J.G.; Frenzel, U.; Kohl, F.J.; Weskamp, T.; Rooney, J.J.; Herrmann, W.A.; Nuyken, O. *J. Organomet. Chem.* **2000**, *606*, 8. (c) Lin, W.-Y.; Wang, H.-W.; Liu, Z.-C.; Xu, J.; Chen, C.-W.; Yang, Y.-C.; Huang, S.-L.; Yang, H.-

C.; Luh, T.-Y. *Chem. Asian J.* **2007**, *2*, 764.

(33) (a) Vehlow, K.; Wang, D.; Buchmeiser, M. R.; Blechert, S. *Angew. Chem. Int. Ed.* **2008**, *47*, 2615. (b) Lichtenheldt, M.; Wang, D.; Vehlow, K.; Reinhardt, I.; Kühnel, C.; Decker, U.; Blechert, S.; Buchmeiser, M. R. *Chem. Eur. J.* **2009**, *15*, 9451. (c) Torker, S.; Müller, A.; Chen, P. *Angew. Chem. Int. Ed.* **2010**, *49*, 3762. (d) Buchmeiser, M. R.; Ahmad, I.; Gurram, V.; Kumar, P. S. *Macromolecules* **2011**, *44*, 4098.

(34) **Poly-6.38** with *cis* content as high as 81% has been previously reported, albeit in very low conversion. See : Ledoux, N.; Allaert, B.; Verpoort, F. *Eur. J. Inorg. Chem.* **2007**, 5578.

(35) Teo, P.; Grubbs, R. H. *Organometallics* **2010**, *29*, 6045.

(36) The *cis* content of **poly-6.38** did not change when the structurally related (H2IMes)Cl2Ru(=CH-*o*-iPr-Ph) and (H2IMes)Cl2Ru(C5H5N)2 were used as catalysts in place of **6.B**. This should not be surprising since all three catalysts initiate to give the same propagating species.

(37) The initiation rate constants of **6.B** and **6.24** are $4.6 \times 10^{-4} \text{ s}^{-1}$ and $8.4 \times 10^{-4} \text{ s}^{-1}$ respectively. Both these values are significantly smaller than the initiation rate constant of (H2IMes)Cl2Ru(C5H5N)2 ($>0.2 \text{ s}^{-1}$), which is the preferred catalyst for ROMP. Note that the initiation rate constant of **6.24** depends on olefin concentration. See the following for a discussion of initiation in ruthenium metathesis catalysts: (a) Sanford, M. S.; Love, J. A.; Grubbs, R. H. *J. Am. Chem. Soc.* **2001**, *123*, 6543. (b) Love, J. A.; Morgan, J. P.; Trnka, T. M.; Grubbs, R. H. *Angew. Chem. Int. Ed.* **2002**, *41*, 4035.

(38) Schleyer, P. v. R.; Williams, J.E.; Blanchard, K.R. *J. Am. Chem. Soc.* **1970**, *92*, 2377.

(39) Bielawski, C. W.; Grubbs, R. H. *Angew. Chem. Int. Ed.* **2000**, *39*, 2903.

(40) For examples of *cis*-selective ROMP of **6.47** using tungsten catalysts see:

(a) Oreshkin, I.; Redkina, L.; Kershenbaum, I.; Chernenko, G.; Makovetsky, K.; Tinyakova, E.; Dolgoplosk, B. *Eur. Poly. J.* **1977**, *13*, 447. (b) Ceausescu, E.; Cornilescu, A.; Nicolescu, E.; Popescu, M.; Coca, S.; Cuzmici, M.; Oprescu, C.; Dimonie, M.; Hubca, G.; Teodorescu, M.; Grosescu, R.; Vasilescu, A.; Dragutan, V. *J. Mol. Catal.* **1986**, *36*, 163. (c) Wei, J.; Leonard, J. *Eur. Poly. J.* **1994**, *30*, 999.

(41) Subsequent addition of norbornene to the reaction mixture containing **6.49** and **6.24** gives **poly-6.38** with the same selectivity as obtained in the individual polymerization of **6.38** with **6.24**, thus demonstrating that *cis*-cyclooctene does not decompose or inhibit **6.24**.

(42) Walker, R.; Conrad, R. M.; Grubbs, R. H. *Macromolecules* **2009**, *42*, 599.

(43) (a) Bielawski, C.W.; Scherman, O. A.; Grubbs R. H. *Polymer* **2001**, *42*, 4939. (b) Abdallaoui, I. A.; Semeril, D.; Dixneuf, P. H. *J. Mol. Catal. A : Chem.* **2002**, *182*, 577.

(44) Odian, G. *Principles of Polymerization*, 4th ed.; John Wiley & Sons: Hoboken, NJ, **2004**; pp 238-239.

(45) Pangborn, A. B.; Giardello, M. A.; Grubbs, R. H.; Rosen, R. K.; Timmers, F. J. *Organometallics* **1996**, *15*, 1518

(46) Blum, A. P.; Ritter, T.; Grubbs, R. H. *Organometallics* **2007**, *26*, 2122.

(47) Keitz, B. K.; Endo, K.; Herbert, M. B.; Grubbs, R. H. *J. Am. Chem. Soc.* **2011**,

133, 9686.